at 37°C for 30 min to make the cell membrane permeable to antibodies. Next, the sections were incubated with TT buffer containing anti-S100 mouse (Chemicon, Temecula, CA, USA) or anti-S100 rabbit (Dako, Produktionsvej, Denmark) antibody at a 1 : 2000 dilution, anti-Shh mouse antibody (5E1; Developmental Studies Hybridoma Bank, Iowa City, IA, USA) at a 1 : 500 dilution, anti-BDNF antibody sheep (Chemicon) at a 1 : 1000 dilution, or anti-GDNF rabbit antibody (kindly provided by Dr Carlos Ibanez) at a 1 : 1000 dilution at 4°C overnight, and subsequently incubated at 23°C for 2 h with TT buffer containing Alexa Fluor 488- or 594-labeled anti-rabbit, mouse, or sheep IgG antibodies (Invitrogen, Carlsbad, CA, USA). After series of wash with TT buffer, the fluorescent images were captured using a confocal laser microscope (Leica, Wetzlar, Germany).

Western blotting

The sciatic nerves were homogenized in 200 μL of lysis buffer (50 mM HEPES, pH 7.5, 150 mM NaCl, 1.5 mM $MgCl_2$, 5 mM EGTA, 10% glycerin, 1% Triton X-100, 0.1 mM Na_3VO_4, 10 μg/mL aprotinine, 10 μg/mL leupeptine, and 1 mM phenylmethylsulfonyl fluoride). For the control of Shh western blot, the mouse Shh expression vector (kindly provided by Dr Masato Nakafuku) was transfected to Cos7 cells using Lipofectamine 2000 (Invitrogen). Lysates were then centrifuged at 12 000 *g* for 20 min at 4°C, and the protein concentration of the supernatant fluid was determined with BCA Protein Assay Kit (Pierce, Rockford, IL, USA). The supernatant (20 μg of protein) was electrophoresed in SDS polyacrylamide gels (15–25% for BDNF or 7.5% for neurofilament 160), and then transferred to polyvinylidene difluoride membranes (Millipore, Billerica, MA, USA). The membranes were washed in PBS containing 0.2% Tween 20, and subsequently reacted with anti-Shh antibody (5E1; Developmental Studies Hybridoma Bank, or clone 171001; R&D Systems, Minneapolis, MN, USA), anti-BDNF sheep antibody (Chemicon) at a 1 : 500 dilution, anti-neurofilament 160 mouse antibody (Sigma) at a 1 : 1000 dilution, anti-actin rabbit antibody (Abcam, Cambridge, MA, USA) at a 1 : 1000 dilution, or anti-S100 rabbit antibody (Dako) at 1 : 1000 dilution for 18 h at 4°C, followed sequentially by reactions with peroxidase-conjugated anti-mouse or sheep IgG antibody (Sigma). The labeled proteins were developed using ECL detection reagent (Amersham Biosciences, Piscataway, NJ, USA) and X-ray film.

Schwann cell culture

Sciatic nerves of postnatal day 3 (P3) Wistar rats were removed and dissociated by incubation in 1 mg/mL collagenase for 1 h. The cells were plated and maintained in Dulbecco's modified Eagle's medium containing 10% fetal calf serum, penicillin (50 units/mL), and 100 μg/mL streptomycin. Cytosine arabinoside (10 μM) was added 1 day after initial plating to reduce fibroblast proliferation. After 1 week, cells were incubated in medium containing 2 μM forskolin and 20 μg/mL bovine pituitary extracts for 1 week to promote Schwann cell proliferation, then treated by 1 μg/mL recombinant N-terminal peptide of Shh (ShhN) (R&D Systems) with or without 5 μM cyclopamine for 2 days.

Transcriptional assay of BDNF promoter

BDNF CAT constructs (kindly provided by Dr Tonis Timmusk) have been described before. The promoter domains excised from

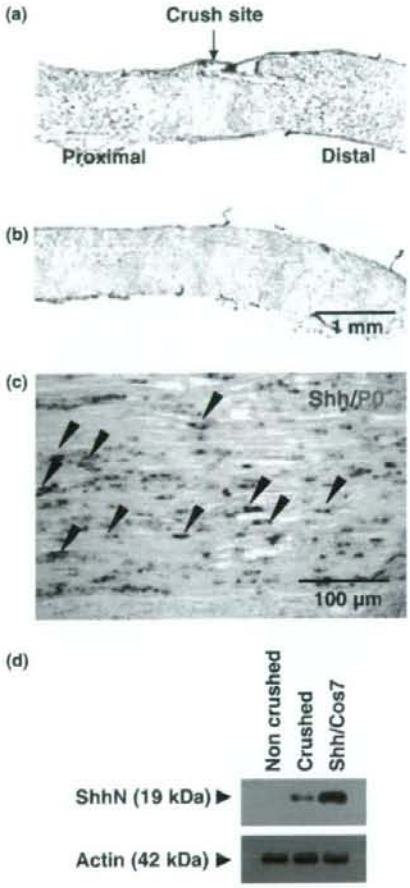

Fig. 1 *In situ* hybridization histochemistry and western blott analysis of Shh in the injured sciatic nerve. Longitudinal sections of the sciatic nerve 1 day after crush (a and c) or non-crush (b) were hybridized with antisense probes for Shh (a and b) or both Shh and P0 (c). Shh was visualized by HistoMark TrueBlue (dark blue in a, b and c), and P0 was by Magenta-phos-*p*-tol (magenta in c). The double-stained Schwann cells were indicated with arrowheads. The section proximal to the injured site shows leftward and distal shows rightward. The sciatic nerve lysate (20 μg) was subjected to western blot analysis. The crushed sciatic nerve expressed the N-terminal Shh protein (d).

BDNF CAT constructs were subcloned to pGL3-Basic luciferase vector (Promega, Madison, WI, USA). The expression vectors for mouse Shh and Smo were kind gifts from Dr Masato Nakafuku. The spontaneously immortalized mice Schwann cell line 32 (IMS32) (Ito *et al.* 2006) was maintained in Dulbecco's modified Eagle's medium with 10% fetal calf serum, penicillin (50 units/mL), and 100 μg/mL streptomycin. One day before transfection, cells were plated at a density of 1×10^5 per 6-well. Lipofectamine 2000 (Invitrogen) was used for transfection according to the manufacturer's instructions. Cells were transfected with 1 μg of luciferase reporter plasmid. For

the co-transfection experiments, we used 0.5 μg of each expression plasmid and 0.2 μg reporter plasmid. The total amount of DNA used for transfection was kept constant at 1.2 μg by addition of empty pcDNA3 vector. In every experiment, 0.1 μg of *Renilla* luciferase plasmid, phRL-Tk vector (Promega) was co-transfected as an internal marker. Forty-eight hours after transfection, cells were lysed and the relative luciferase activity (RLA) was measured with a luminometer (Victor2 1420 MultiLabel counter; Perkin-Elmer, Waltham, MA, USA) by using the dual-luciferase reporter assay system (Promega). All experiments were performed at least three times with different preparations of plasmid DNA. Control transfections were performed to ensure that base reporter vectors were not solely regulated by Shh/Smo.

Results

Up-regulation of Shh mRNA in injured sciatic nerve

The expression of Shh in the injured site was investigated by *in situ* hybridization 1 day after rat sciatic nerve crush. Shh mRNA was detected in the areas proximal and distal to the crush site of the sciatic nerve (Fig. 1a), while not detected in non-crushed sciatic nerve (Fig. 1b). Double *in situ* hybridization showed that the dark blue staining (HistoMark TrueBlue) of Shh co-localized with the magenta staining (Magenta-phos-*p*-tol) corresponded to P0, a specific marker for Schwann cells (arrowheads in Fig. 1c). To confirm up-regulated expression of Shh, the lysate from sciatic nerve was subjected to the western blot analysis using anti-Shh antibody specifically reacts with N-terminal of Shh. The crushed sciatic nerve expressed the band of 20kDa that was the same molecular size of transfected Shh. These findings suggest that Shh mRNA was expressed in Schwann cells around the injured site of the sciatic nerve.

Injury-induced mRNA expression of Shh, Gli1, BDNF, and GDNF

Time-dependent mRNA expression of Shh, Gli1, BDNF, and GDNF was examined in the segment proximal or distal to the crush site of the rat sciatic nerve (Fig. 2). All mRNAs examined were significantly up-regulated after injury, and the degree of their increases was larger in distal segments regardless of time after injury. Shh mRNA level started to increase 12 h after crush and peaked at 1–3 days. Gli1 mRNA level significantly elevated 3 days to 1 week after injury. Up-regulation of BDNF mRNA was observed only

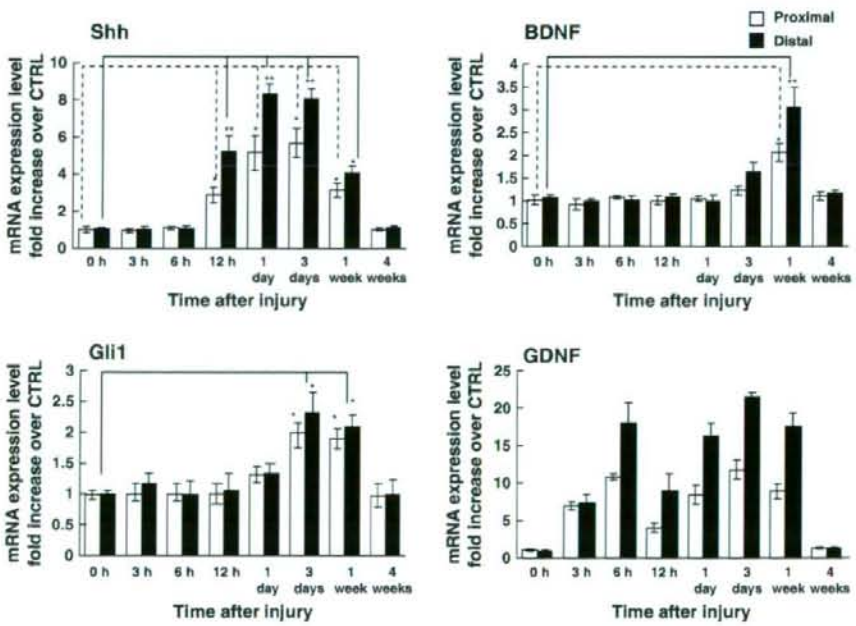

Fig. 2 Time course of Shh-, Gli1-, BDNF-, and GDNF-mRNA expression of after sciatic nerve injury. Total RNA of the segment proximal or distal to the injured site of the sciatic nerve was subjected to real-time PCR using primers specific for the respective target genes. The values are expressed as the mean ± SE ($n = 3$) of the fold-increase over the contralateral non-injured segment of the sciatic nerve. Significant differences from the value of the corresponding control group were determined by one-way ANOVA and Tukey test. Significance, $^{*}p < 0.05$, $^{**}p < 0.01$. CTRL, control.

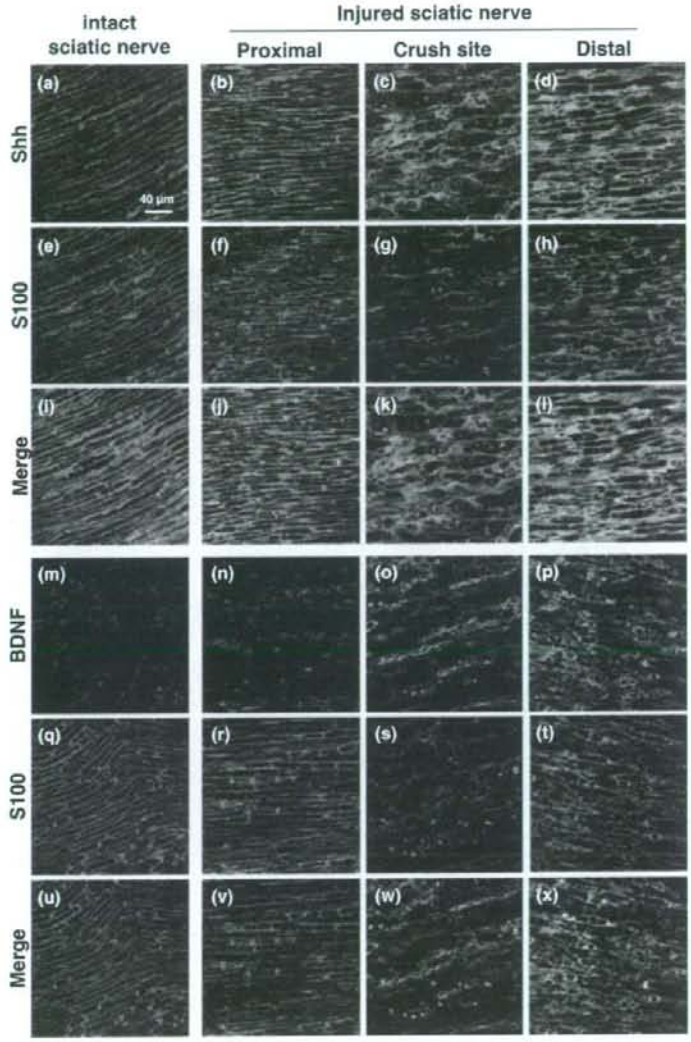

Fig. 3 Localization of Shh and BDNF immunoreactivities in the injured sciatic nerve. Longitudinal sections of intact sciatic nerve (a, e, i, m, q, and u) or sciatic nerve 1 week after injury were reacted with anti-Shh (a–d) and anti-S100 (e–h) antibody, and respectively visualized by Alexa-Fluor 488-conjugated (green) and Alexa-Fluor 594-conjugated (red) secondary antibody. The sections proximal (b, f, j, n, r, and v) or distal (d, h, l, p, t, and x) to crush site are the area 4 mm distant from the center of the crush site. Scale bar: 40 μm.

1 week after injury. The pattern of time-dependent mRNA expression of GDNF was two phases. The first peak was 6 h after injury, and the second peak was 3 days. Expression of four mRNAs returned to basal levels 4 weeks after injury. Thus, the increase of Shh mRNA was followed by that of Gli1, BDNF, and GDNF. This result implies the possibility that Shh regulates the expression of BDNF and GDNF such as Gli1.

Expression of Shh and BDNF in injured sciatic nerve

Characterization of cells producing Shh and BDNF in sciatic nerve 1 week after injury was immunohistochemically analyzed. The expression of BDNF and GDNF were previously reported in Schwann cells of injured nerves (Hammarberg *et al.* 1996; Zhang *et al.* 2000). We examined the double staining of Shh and labeling of S100, a protein specific for Schwann cells. Shh was up-regulated in every segment of injured sciatic nerve, especially in the distal segment (Fig. 3a–d). Its expression was observed in S100-positive cells (Fig. 3i–l). Expression of BDNF was robustly induced in crush site and distal segment (Fig. 3p), and localized in S100-positive cells of the distal segment of injured sciatic nerve (Fig. 3x). These results show that the major cells producing Shh and BDNF after sciatic nerve injury are Schwann cells in distal segment. We also analyzed the GDNF immunoreactivity. The distal segment of injured

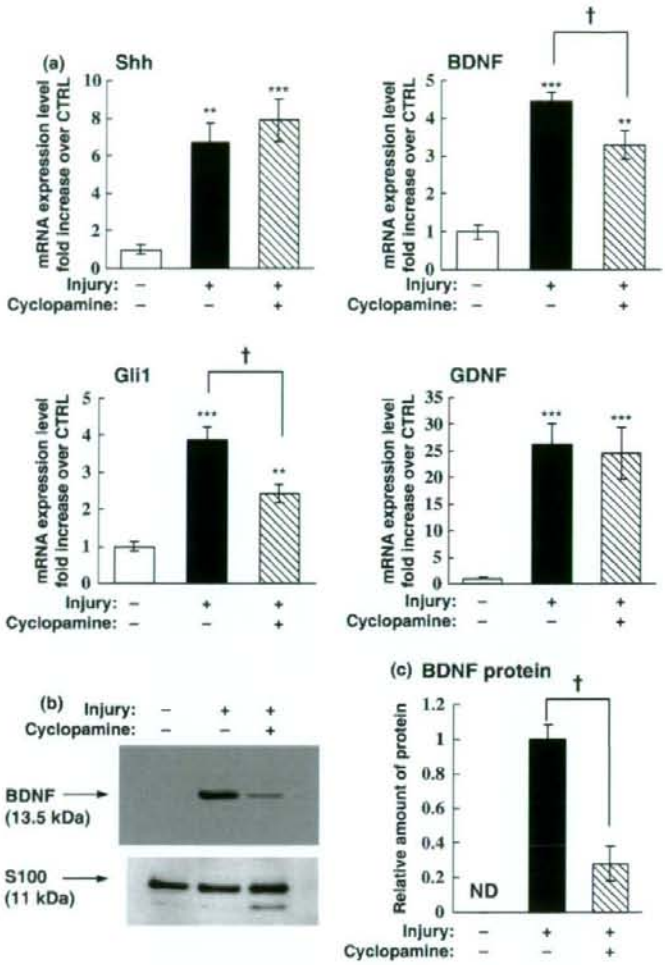

Fig. 4 Alteration of BDNF expression by Shh signaling inhibition after sciatic nerve injury. (a and b) Shh-, Gli1-, BDNF-, and GDNF-mRNA expression at 1 week after continuous administration of cyclopamine, hedgehog signaling inhibitor, was analyzed by real-time PCR. The values are expressed as the mean ± SE ($n = 4$) of the fold-increase over the non-treated sciatic nerve. (c) An amount of BDNF protein was analyzed by western blotting. The bands of 13.5 kDa BDNF protein were densitometrically quantified. The values are expressed as the mean ± SE ($n = 4$) of the fold-increase over the vehicle-administered sciatic nerve after injury. Significant differences were determined by Student's *t*-test, $^{**}p < 0.01$, $^{***}p < 0.001$ versus the non-treated group, $\dagger p < 0.05$ versus the nerve injury plus vehicle group. ND, not detectable. CTRL, control.

sciatic nerve expressed high level of GDNF immunoreactivity as shown in Supporting information Fig. S1d and l.

Effect of Shh signaling inhibition on expression of neurotrophic factors after sciatic nerve injury

To investigate whether Shh regulates the expression of BDNF and GDNF after sciatic nerve injury, cyclopamine, Shh signaling inhibitor (Chen *et al.* 2002) or 45% HBC (vehicle) was continuously administered to injured site of sciatic nerve by osmotic pumps for 1 week. Then, the mRNA expression of Shh, Gli1, BDNF, and GDNF in injured site treated by cyclopamine was compared with that in injured site injected vehicle using real-time PCR analysis. Inhibition of Shh signaling by continuous administration of cyclopamine decreased the mRNA up-regulation of Gli1 and BDNF after injury, but did not affect that of Shh and GDNF (Fig. 4a). The reduction of Gli1 expression by cyclopamine agrees with previous findings (Lamm *et al.* 2002; Turner *et al.* 2006). BDNF expression after administration of cyclopamine following injury was also decreased at the protein level (Fig. 4b and c). These results suggest that Shh signaling regulates BDNF expression as well as Gli1 after sciatic nerve injury.

Survival of motor neurons by Shh signaling inhibition

The effect of Shh signaling inhibition on survival of motor neurons after sciatic nerve injury was investigated. Neurons in L4-5 spinal cord 1 week after sciatic nerve injury were labeled by Nissl staining (Fig. 5a). Motor neurons in the ventral horn were defined as Nissl-positive cell with the cell body over 20 μm, and counted. The number of motor neurons in the vehicle-administered side of a section was 14.9 ± 0.95 cells; meanwhile the number in the cyclopamine-administered side was 11.0 ± 1.01 cells. The motor

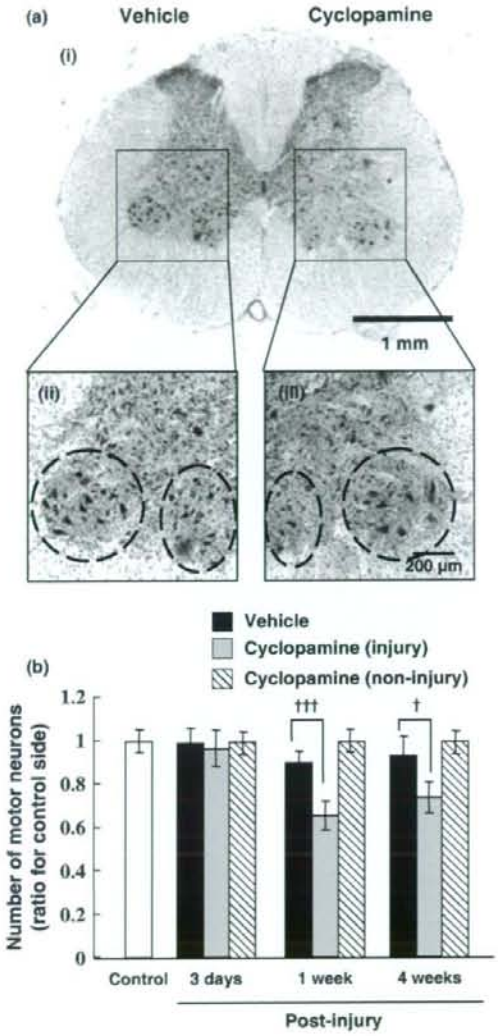

Fig. 5 Effect of cyclopamine on survival of motor neurons after sciatic nerve injury. Coronal sections of the L4-5 spinal cord 1 week after continuous administration of vehicle or cyclopamine to injury site following sciatic nerve injury were Nissl-stained for labeling of neurons (a-i). Box in a-i indicates the high magnification of the ventral horns of the vehicle- (a-ii) or cyclopamine- (a-iii) injected side. Circle in a-ii and a-iii indicates the motor neuron-existing area. Motor neuron was defined as a Nissl-positive cell with the cell body over 20 μm diameter, and counted in a section (b). The values are expressed as the mean ± SE ($n = 4$) of the fold-increase over the number of motor neurons of the vehicle side. The empty box indicated the number of motor neurons with cyclopamine treatment in non-injury sciatic nerve. Significant differences from the value of the vehicle side were determined by Student's *t*-test, †††$p < 0.001$, †$p < 0.05$.

neurons were significantly decreased by continuous cyclopamine treatment after sciatic nerve injury (Fig. 5b). Injection of cyclopamine to non-injured sciatic nerve did not influence the survival of the motor neurons, showing cyclopamine itself has no neurotoxic effect. This demonstrates that Shh induced in the injured sciatic nerve may play a neuroprotective role for motor neurons. In the regard of axonal regeneration, we tested whether cyclopamine may influence the neurofilament expression that corresponds the degree of axonal regeneration. The continuous administration of cyclopamine did not change the neurofilament expression as shown in supporting information Fig. S2.

Effect of Shh on cultured Schwann cells

To investigate whether BDNF expression in Schwann cells is actually enhanced by Shh signaling, we used primary Schwann cells from P3 rat sciatic nerves. The purity of the Schwann cells used in this study was determined by immunohistochemical staining of S100 and counterstaining by 4′,6-diamidino-2-phenylindole (DAPI) (Fig. 6a), and was consequently more than 95%. Next, we found that the cultured Schwann cells express Shh receptors, Ptc1 and Smo (Fig. 6b), suggesting the possibility that the Schwann cells may respond to Shh. Based on these findings, the effects of Shh in the cultured Schwann cells were examined. The cells were treated by 1 μg/mL N-terminal peptide of Shh (ShhN: the active form of Shh) for 2 days, resulting in the up-regulation of BDNF mRNA as well as Gli1 mRNA. Their up-regulation was suppressed by cotreatment of cyclopamine. For further quantification of this result, the real-time PCR was performed (Fig. 6c). The expression of Gli1 and BDNF was significantly up-regulated in cultured Schwann cells when Shh was added. This stimulus had no effects on GDNF expression. These results suggest that Shh signaling increases the BDNF expression in Schwann cells.

Next we tested whether Shh regulates BDNF promoter activities by using the luciferase reporter assay. We used the immortalized Schwann (IMS32) cells because the primary Schwann cell culture is resistant for the lipofection. Because the RT-PCR experiment showed that IMS32 cells expressed the low level of Smo compared to Ptc1 (data not shown), we co-transfected Smo in combination with Shh. The BDNF promoter activity was significantly higher when Shh and Smo were co-transfected compared to the mock vector transfection (Fig. 7). The RLA was significantly higher in the luciferase vector containing the exon I and II of BDNF gene (about five-fold).

Discussion

We found that the up-regulated expression of Shh in the Schwann cells of the crushed sciatic nerve was followed by that of Gli1, BDNF and GDNF. The time-course of Shh, BDNF and GDNF expression was consistent with

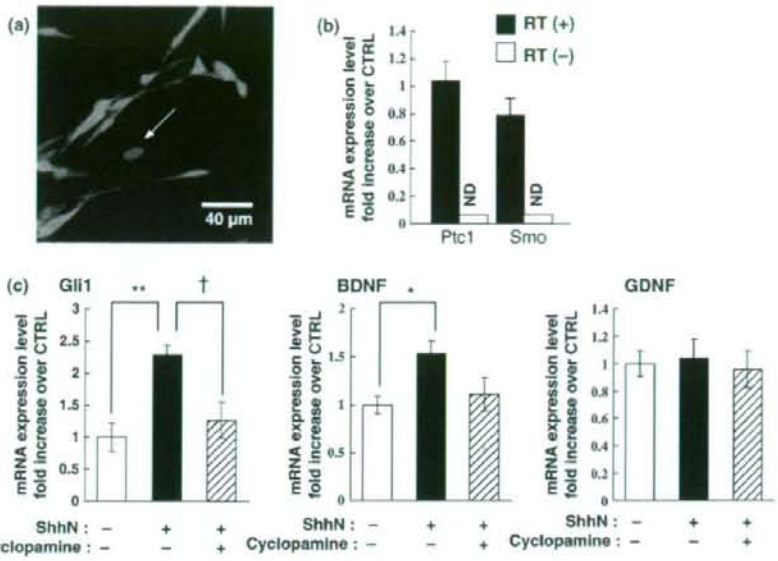

Fig. 6 BDNF mRNA up-regulation induced by Shh in cultured Schwann cells. (a) Primary Schwann cells from P3 rat sciatic nerves were stained with anti-S100 antibody (red), and cell nuclei were visualized with DAPI (blue). Arrow indicates a S100-negative cell, presumably a fibroblast. (b) Expression of Ptc1 and Smo in cultured Schwann cells was investigated by real-time PCR comparing GADPH as a control, showing that the Schwann cells had Ptc1 and Smo (*RT+*). No amplification was obtained (ND) when the RT reaction was performed without reverse transcriptase (*RT-*). (c) mRNA expression of Gli1, BDNF, and GDNF in the Schwann cells treated by 1 μg/mL ShhN with or without 5 μM cyclopamine for 2 days was analyzed by RT-PCR. The fold increase over non-treated control ($2^{-\Delta\Delta Ct}$) was analyzed by the real-time RT-PCR. Significant differences were determined by Student's *t*-test, $^{*}p < 0.05$, $^{**}p < 0.01$ versus the non-treated group, $^{\dagger}p < 0.05$ versus the ShhN-treated group. CTRL, control.

previous findings (Meyer *et al.* 1992; Hoke *et al.* 2000; Yamada *et al.* 2004; Xu *et al.* 2008). Our starting and working hypothesis was that the expression of BDNF and GDNF after nerve injury might be somehow linked with Shh. To examine the roles of Shh signaling, we applied cyclopamine to the injury sites. Cyclopamine is a steroid-alkaloid that inhibits the hedgehog signaling through interaction with the hedgehog receptor Smo (Chen *et al.* 2002). Therefore, it is possible that cyclopamine may also inhibit the signaling of desert hedgehog (Dhh) and Indian hedgehog (Ihh), other members of the hedgehog family. However, the previous report showed that Dhh is down-regulated and disappears in Schwann cells after the sciatic nerve injury (Bajestan *et al.* 2006). Therefore, these results highly indicated that the cyclopamine administration to the injury sites predominantly inhibits the signaling of Shh, not that of Dhh or Ihh.

Previously Gli1 has been reported as a transcription factor regulated by Shh signaling (Lamm *et al.* 2002; Turner *et al.* 2006). Here, we found the decrease of the Gli1 expression in the sciatic nerves, suggesting that the continuous administration of cyclopamine inhibited the Shh signaling at the injury site. We next observed the BDNF expression was also reduced by cyclopamine, meanwhile the GDNF expression was not influenced. These results implied that BDNF may be somehow regulated by the Shh signaling. To test our hypothesis, we used the cultured Schwann cells. The expression of BDNF as well as Gli1 was induced by the Shh application to the culture medium, while there was no change in the GDNF expression. To further confirm that Shh signaling may regulate BDNF transcription, we used the luciferase reporter assay. The BDNF gene consists of four short 5′-exons (I–IV) and one 3′-exon (V) which encodes the BDNF protein. Timmunsk *et al.* have shown that the usage of these exons and their regulated expression comprise the tissue specific expression of BDNF, for example, mRNAs containing exons I, II, or III are predominantly expressed in the brain, and exon IV in the lung and heart (Timmusk *et al.* 1993). Our data indicated that BDNF promoter containing exon I and II predominates in the IMS32 cells, responding to the Shh signaling. Recent report described that Shh negatively regulate the nerve growth factor mRNA in developing somites (Cotrina *et al.* 2000). Although the precise mechanisms how Shh signaling can regulate the BDNF and nerve growth factor still remain unclear, these results will draw a new attention to the signal linkage between Shh and neurotrophines.

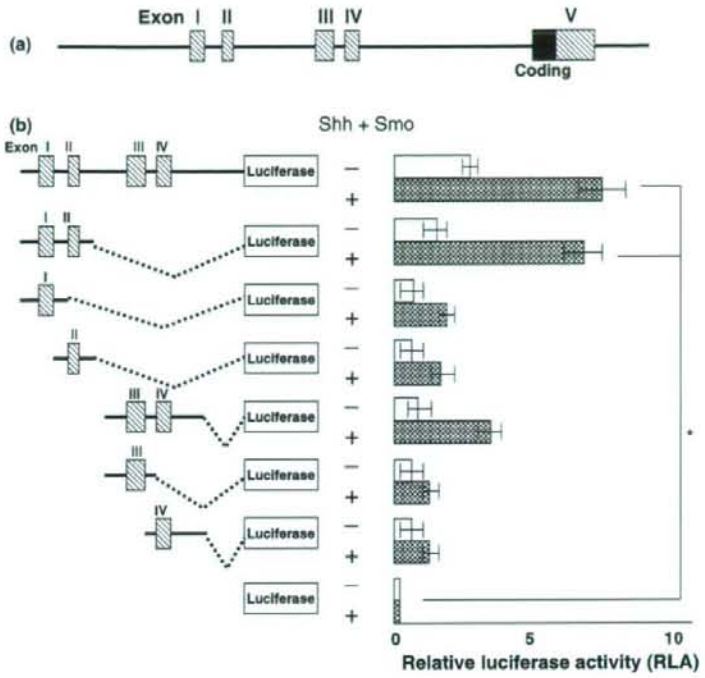

Fig. 7 Activation of BDNF promoter in IMS32 cells co-transfected with Shh and Smo. (a) The schematic diagram showing the rat BDNF gene and the six luciferase reporter constructs. The promoter activity in the presence of Shh and Smo was shown as a relative luciferase activity (RLA) ($n = 3$). Significant differences were determined by Student's *t*-test, $^*p < 0.001$ versus the luciferase activity without BDNF promoter.

The possibility that the pathological status may alter the BDNF expression was first suggested from the observation that the BDNF expression was dramatically increased in the neocortex following experimentally induced seizures (Ernfors *et al.* 1991). Other stimulus that clearly resulted in neurodegeneration, such as traumatic injury, ischemia, and hypoglycemia, also change the BDNF expression (Lindvall *et al.* 1994). BDNF levels remained elevated throughout myelination of Schwann cells through $p75^{NTR}$ (Cosgaya *et al.* 2002). The present result is the first report that the BDNF up-regulation after nerve injury is mutually linked with the elevated level of Shh.

In cultured Shcwann cells, the expression of Smo is relatively weaker than that of Ptc1 (Fig. 6b). This is the reason why we co-transfected Shh and Smo to regulate BDNF reporter activity. However, in our sciatic nerve injury experiments, Smo transcripts were detected in the injury site, while Ptc1 transcripts were not (data not shown). This is the same result as we previously reported in the case of facial nerve axotomy (Akazawa *et al.* 2004). It has not been fully elucidated how Shh may work in the local pathway. One of the possible explanations is the involvement of other types of cells in injury site, such as inflammatory cells and fibroblasts. There is a clear discrepancy that Shh was up-regulated in both proximal and distal segments, while BDNF is only up-regulated in the distal. We need to consider the other cellular or molecular pathway that mediates the signaling between Shh and BDNF. Even in the cultured Schwann cells, 5% of total cells showed S100 negative (Fig. 7a). Although the experiments presented here has some issues that have to be addressed, it is our goal to understand the mechanisms of the Shh-BDNF signal in detail. Further studies will be required to confirm the mode of Shh signaling and how Shh may regulate the BDNF transcription.

Acknowledgments

Authors thank members of Kohsaka's lab and Akazawa's lab for technical help and discussion. This work was supported by the grants from Ministry of Health, Labour and Welfare, Japan and Ministry of Education, Culture, Sports, Science and Technology, Japan.

Supporting information

Additional Supporting Information may be found in the online version of this article:

Table S1 The specific primers used for Shh, Gli1, BDNF, GDNF, Ptc1, Smo, and GAPDH.

Fig. S1 The GDNF immunoreactivity was examined in the injured sciatic nerve.

Fig. S2 We tested whether Shh signaling after nerve injury affects axonal regeneration.

References

Akazawa C., Tsuzuki H., Nakamura Y., Sasaki Y., Ohsaki K., Nakamura S., Arakawa Y. and Kohsaka S. (2004) The upregulated expression of sonic hedgehog in motor neurons after rat facial nerve axotomy. *J. Neurosci.* **24**, 7923–7930.

Aszmann O. C., Korak K. J., Kropf N., Fine E., Aebischer P. and Frey M. (2002) Simultaneous GDNF and BDNF application leads to increased motoneuron survival and improved functional outcome in an experimental model for obstetric brachial plexus lesions. *Plast. Reconstr. Surg.* **110**, 1066–1072.

Bajestan S. N., Umehara F., Shirahama Y., Itoh K., Sharghi-Namini S., Jessen K. R., Mirsky R. and Osame M. (2006) Desert hedgehog-patched 2 expression in peripheral nerves during Wallerian degeneration and regeneration. *J. Neurobiol.* **66**, 243–255.

Berman D. M., Karhadkar S. S., Maitra A. *et al.* (2003) Widespread requirement for Hedgehog ligand stimulation in growth of digestive tract tumours. *Nature* **425**, 846–851.

Briscoe J., Sussel L., Serup P., Hartigan-O'Connor D., Jessell T. M., Rubenstein J. L. and Ericson J. (1999) Homeobox gene Nkx2.2 and specification of neuronal identity by graded Sonic hedgehog signalling. *Nature* **398**, 622–627.

Chen J. K., Taipale J., Cooper M. K. and Beachy P. A. (2002) Inhibition of Hedgehog signaling by direct binding of cyclopamine to Smoothened. *Genes Dev.* **16**, 2743–2748.

Cosgaya J. M., Chan J. R. and Shooter E. M. (2002) The neurotrophin receptor p75NTR as a positive modulator of myelination. *Science (New York, NY)* **298**, 1245–1248.

Cotrina M. L., Gonzalez-Hoyuela M., Barbas J. A. and Rodriguez-Tebar A. (2000) Programmed cell death in the developing somites is promoted by nerve growth factor via its p75(NTR) receptor. *Dev. Biol.* **228**, 326–336.

Ernfors P., Bengzon J., Kokaia Z., Persson H. and Lindvall O. (1991) Increased levels of messenger RNAs for neurotrophic factors in the brain during kindling epileptogenesis. *Neuron* **7**, 165–176.

Friedman B., Kleinfeld D., Ip N. Y., Verge V. M., Moulton R., Boland P., Zlotchenko E., Lindsay R. M. and Liu L. (1995) BDNF and NT-4/5 exert neurotrophic influences on injured adult spinal motor neurons. *J. Neurosci.* **15**, 1044–1056.

Funakoshi H., Frisen J., Barbany G., Timmusk T., Zachrisson O., Verge V. M. and Persson H. (1993) Differential expression of mRNAs for neurotrophins and their receptors after axotomy of the sciatic nerve. *J. Cell Biol.* **123**, 455–465.

Hahn H., Wojnowski L., Miller G. and Zimmer A. (1999) The patched signaling pathway in tumorigenesis and development: lessons from animal models. *J. Mol. Med.* **77**, 459–468.

Hammarberg H., Piehl F., Cullheim S., Fjell J., Hokfelt T. and Fried K. (1996) GDNF mRNA in Schwann cells and DRG satellite cells after chronic sciatic nerve injury. *Neuroreport* **7**, 857–860.

Hoke A., Cheng C. and Zochodne D. W. (2000) Expression of glial cell line-derived neurotrophic factor family of growth factors in peripheral nerve injury in rats. *Neuroreport* **11**, 1651–1654.

Houenou L. J., Oppenheim R. W., Li L., Lo A. C. and Prevette D. (1996) Regulation of spinal motoneuron survival by GDNF during development and following injury. *Cell Tissue Res.* **286**, 219–223.

Ito Y., Wiese S., Funk N., Chittka A., Rossoll W., Bommel H., Watabe K., Wegner M. and Sendtner M. (2006) Sox10 regulates ciliary neurotrophic factor gene expression in Schwann cells. *Proc. Natl Acad. Sci. USA* **103**, 7871–7876.

Lamm M. L., Catbagan W. S., Laciak R. J., Barnett D. H., Hebner C. M., Gaffield W., Walterhouse D., Iannaccone P. and Bushman W. (2002) Sonic hedgehog activates mesenchymal Gli1 expression during prostate ductal bud formation. *Dev. Biol.* **249**, 349–366.

Lindvall O., Kokaia Z., Bengzon J., Elmer E. and Kokaia M. (1994) Neurotrophins and brain insults. *Trends Neurosci.* **17**, 490–496.

Loers G. and Schachner M. (2007) Recognition molecules and neural repair. *J. Neurochem.* **101**, 865–882.

Meyer M., Matsuoka I., Wetmore C., Olson L. and Thoenen H. (1992) Enhanced synthesis of brain-derived neurotrophic factor in the lesioned peripheral nerve: different mechanisms are responsible for the regulation of BDNF and NGF mRNA. *J. Cell Biol.* **119**, 45–54.

Richardson W. D., Pringle N. P., Yu W. P. and Hall A. C. (1997) Origins of spinal cord oligodendrocytes: possible developmental and evolutionary relationships with motor neurons. *Dev. Neurosci.* **19**, 58–68.

Riobo N. A., Lu K. and Emerson Jr C. P. (2006) Hedgehog signal transduction: signal integration and cross talk in development and cancer. *Cell Cycle* **5**, 1612–1615.

Soula C., Danesin C., Kan P., Grob M., Poncet C. and Cochard P. (2001) Distinct sites of origin of oligodendrocytes and somatic motoneurons in the chick spinal cord: oligodendrocytes arise from Nkx2.2-expressing progenitors by a Shh-dependent mechanism. *Development* **128**, 1369–1379.

Stone D. M., Hynes M., Armanini M. *et al.* (1996) The tumour-suppressor gene patched encodes a candidate receptor for Sonic hedgehog. *Nature* **384**, 129–134.

Timmusk T., Palm K., Metsis M., Reintam T., Paalme V., Saarma M. and Persson H. (1993) Multiple promoters direct tissue-specific expression of the rat BDNF gene. *Neuron* **10**, 475–489.

Turner T. T., Bang H. J., Attipoe S. A., Johnston D. S. and Tomsig J. L. (2006) Sonic hedgehog pathway inhibition alters epididymal function as assessed by the development of sperm motility. *J. Androl.* **27**, 225–232.

te Welscher P., Zuniga A., Kuijper S., Drenth T., Goedemans H. J., Meijlink F. and Zeller R. (2002) Progression of vertebrate limb development through SHH-mediated counteraction of GLI3. *Science (New York, NY)* **298**, 827–830.

Winer J., Jung C. K., Shackel I. and Williams P. M. (1999) Development and validation of real-time quantitative reverse transcriptase-polymerase chain reaction for monitoring gene expression in cardiac myocytes in vitro. *Anal. Biochem.* **270**, 41–49.

Xie J., Murone M., Luoh S. M. *et al.* (1998) Activating Smoothened mutations in sporadic basal-cell carcinoma. *Nature* **391**, 90–92.

Xu Q. G., Midha R., Martinez J. A., Guo G. F. and Zochodne D. W. (2008) Facilitated sprouting in a peripheral nerve injury. *Neuroscience* **152**, 877–887.

Yamada Y., Shimizu K., Nitta A., Soumiya H., Fukumitsu H. and Furukawa S. (2004) Axonal regrowth downregulates the synthesis of glial cell line-derived neurotrophic factor in the lesioned rat sciatic nerve. *Neurosci. Lett.* **364**, 11–15.

Zhang J. Y., Luo X. G., Xian C. J., Liu Z. H. and Zhou X. F. (2000) Endogenous BDNF is required for myelination and regeneration of injured sciatic nerve in rodents. *Eur. J. Neurosci.* **12**, 4171–4180.

J Neuropathol Exp Neurol

Vol. 67, No. 6
June 2008
pp. 565–577

ORIGINAL ARTICLE

Neurologic Phenotype of Schimke Immuno-Osseous Dysplasia and Neurodevelopmental Expression of SMARCAL1

Kimiko Deguchi, MD, PhD, Johanna M. Clewing, MD, Leah I. Elizondo, Ryuki Hirano, MD, PhD, Cheng Huang, MD, PhD, Kunho Choi, MS, Emily A. Sloan, Thomas Lücke, MD, Katja M. Marwedel, MD, Ralph D. Powell Jr, MD, Karen Santa Cruz, MD, Sandrine Willaime-Morawek, PhD, Ken Inoue, MD, PhD, Shu Lou, MD, Jennifer L. Northrop, MD, PhD, Yonehiro Kanemura, MD, PhD, Derek van der Kooy, PhD, Hideyuki Okano, MD, PhD, Dawna L. Armstrong, MD, and Cornelius F. Boerkoel, MD, PhD

Abstract

Schimke immuno-osseous dysplasia (OMIM 242900) is an uncommon autosomal-recessive multisystem disease caused by mutations in *SMARCAL1* (swi/snf-related, matrix-associated, actin-dependent regulator of chromatin, subfamily a-like 1), a gene encoding a putative chromatin remodeling protein. Neurologic manifestations identified to date relate to enhanced atherosclerosis and cerebrovascular disease. Based on a clinical survey, we determined that half of Schimke immuno-osseous dysplasia patients have a small head circumference, and 15% have social, language, motor, or cognitive abnormalities. Postmortem examination of 2 Schimke immuno-osseous dysplasia patients showed low brain weights and subtle brain histologic abnormalities suggestive of perturbed neuron-glial migration such as heterotopia, irregular cortical thickness, incomplete gyral formation, and poor definition of cortical layers. We found that SMARCAL1 is highly expressed in the developing and adult mouse and human brain, including neural precursors and neuronal lineage cells. These observations suggest that SMARCAL1 deficiency may influence brain development and function in addition to its previously recognized effect on cerebral circulation.

Key Words: Immunodeficiency, Microcephaly, Neural stem cell, Neuronal migration, Renal disease, Skeletal dysplasia

From the Departments of Pathology (KD, DLA) and Molecular and Human Genetics (KD, JMC, CH, EAS, SL, JLN), Interdepartmental Program in Cell and Molecular Biology (LIE), Baylor College of Medicine, Houston, Texas; Centre for Molecular Medicine and Therapeutics (LIE, RH, KC, CFB), Child and Family Research Institute, Department of Medical Genetics, University of British Columbia, Vancouver, Canada; Departments of Pediatrics (TL) and Pathology (KMM), Hannover Medical School, Hannover, Germany; Department of Laboratory Medicine and Pathology (RDP, KSC), University of Minnesota, Minneapolis, Minnesota; Department of Physiology (HO), Keio University School of Medicine, Tokyo, Japan; Department of Medical Genetics and Microbiology (SWM, DK), University of Toronto, Donnelly Centre for Cellular Department of Mental Retardation and Birth Defect Research (KI), National Institute of Neuroscience, National Center of Neurology and Psychiatry, Tokyo; and Institute for Clinical Research (YK), Osaka National Hospital, National Hospital Organization, Osaka, Japan.

Send correspondence and reprint requests to: Cornelius F. Boerkoel, MD, PhD, University of British Columbia, Department of Medical Genetics, Children's and Women's Health Centre of BC, 4500 Oak St., Rm. C234, Vancouver, British Columbia, Canada V6H 3N1; E-mail: boerkoel@interchange.ubc.ca

The authors Deguchi and Clewing contributed equally to this article.

This work was supported in part by grants from the National Institute of Diabetes, Digestive, and Kidney Diseases, National Institutes of Health (to C.F.B. and D.L.A), the March of Dimes (to C.F.B.), the Gillson Longenbaugh Foundation (to C.F.B), Grant No. P03HD24064 from the New Development Award, Microscopy, and Administrative Cores of the MRDDRC (to C.F.B. and D.L.A.), the Canadian Stem Cell Network (to S.W-M.), the Canadian Institutes for Health Research (to D.V.), the Project for Realization of Regenerative Medicine from Ministry of Education, Culture, Sports, Science and Technology, Japan (to H.O.), the Japan Science and Technology Corporation (CREST; to H.O.), the National Institutes of Health (Birth Defects Laboratory at the University of Washington), and Grant No. H18-Kokoro-Ippan-015 from the Health and Labor Science Research Grant, Japan (to K.D. and K.I.).

Supplemental Materials and Methods data and Supplementary Figures 1–3 are available online at http://www.jneuropath.com.

INTRODUCTION

Neurons of the central nervous system (CNS) originate from the neural precursors within the neuroepithelium surrounding the developing ventricles. The neuronal or glial destiny of the precursors is partly dependent on the number of preceding cell cycles (1). Neurons arise more frequently when the precursor has completed fewer cell divisions, whereas glia arise more frequently when the precursor has completed a higher number of cell divisions (2, 3). Additionally, symmetric or asymmetric cell division determines whether both progeny of a neural precursor remain precursors or whether 1 daughter cell will become a neuron or glia and 1 daughter cell will remain as a neural precursor (2, 4).

The migration of neuronal precursors from the neuroepithelium is carefully choreographed to form cortical layers 2 to 6 (5). A major population of neuronal precursors is guided to the cortex by climbing radial glial fibers (6). The cerebral cortex is formed by an inside-out migration; thus, neurons generated early in cortical development occupy more proximal or internal layers, and those generated later occupy more distal or external layers (7). Neuronal migration can be divided into several key stages according to mutations identified in human diseases: initiation of migration, effective migration, and penetration of the subplate (8).

Schimke immuno-osseous dysplasia (SIOD; OMIM 242900) is an uncommon autosomal-recessive multisystem disease caused by mutations in the putative chromatin remodeling protein SMARCAL1 (swi/snf-related, matrix-associated, actin-dependent regulator of chromatin, subfamily a-like 1). Clinical studies of SIOD have suggested that this multisystem disease is the result of a defect in selective cellular proliferation because its phenotype includes short stature from impaired chondrogenesis, T-cell deficiency from impaired T-cell proliferation, azoospermia from testicular hypoplasia, and, occasionally, bone marrow failure from impaired blood precursor proliferation (9, 10). Other aspects of SIOD are also consistent with impaired differentiation and tissue maintenance and include progressive atherosclerosis leading to cerebral ischemic lesions, renal failure from focal segmental glomerulosclerosis, and fatty infiltration of the right ventricular wall resembling an arrhythmogenic right ventricular cardiomyopathy (9, 10). SMARCAL1 is homologous to the SNF2 chromatin remodeling proteins and the SF2 family of helicases (11, 12). In vitro, SMARCAL1 has DNA-dependent adenosine triphosphatase activity and binds nucleosomes (12, 13), but its in vivo function has not been defined.

In this study, we investigated possible roles of SMARCAL1 in CNS development by characterizing non-ischemic brain pathology in autopsy tissue from 2 patients with SIOD. Both patients had a reduced brain weight and subtle microscopic findings suggestive of malformative processes. To explore the possible implications of these developmental brain lesions, we examined the records of 33 SIOD patients with SMARCAL1 mutations for evidence of decreased brain size, psychomotor delay, and seizures. We found that nearly half of SIOD patients had a head circumference at least 2 standard deviations less than the mean, and approximately 15% had social, language, motor, or cognitive abnormalities. To determine whether these functional and morphologic problems might correlate with disordered brain development in SIOD, we analyzed SMARCAL1 expression in human and murine neural development. SMARCAL1 was found to be highly expressed in human and mouse neural precursors and neurons. Thus, the loss of functional SMARCAL1 may affect the regulation of brain development and cause cerebrovascular ischemia in SIOD.

MATERIALS AND METHODS

Human Subjects

Patients referred to this study gave informed consent approved by the institutional review board of Baylor College of Medicine (Houston, TX) or the Hospital for Sick Children (Toronto, Ontario, Canada). The clinical data for patients were obtained from questionnaires completed by the responsible physician and from medical records and summaries provided by that physician. Postmortem tissue samples were obtained from patients whose families gave informed consent approved by the institutional review board of Baylor College of Medicine.

Human brain tissue for Western and Northern analyses was obtained from the Birth Defects Laboratory (University of Washington, Seattle, WA). Human brain tissue for immunohistochemical and immunofluorescent analyses was obtained from autopsy specimens of unaffected individuals aged 6 gestational weeks (GW) to 61 years; these were obtained after informed consent approved by the institutional review board of Baylor College of Medicine and Texas Children's Hospital. The autopsies were performed within 24 hours of death.

Tissue Pathology and Expression Analyses

Two to 4 investigators who were blinded to the source of the tissue samples determined the pathologic findings, identified immunohistochemically positive cells, and scored the numbers of immunohistochemically positive cells. The assessments of human tissue were done in both SIOD patients and in human control samples as described in the Results section. The assessment of Smarcal1 expression in mouse tissue was done using animals of 3 different genetic backgrounds: 129SvEv, C57BL6, and ICR.

Human and Mouse Neurosphere Culture

All experiments using human neural precursor cells that were derived from human fetal neural tissue aged 7 to 10 GW were performed at Keio University with the approval of the institutional review board and in agreement with the ethical guidelines of the ethical committees of Osaka National Hospital and Keio University. Tissue procurement was in accordance with the Declaration of Helsinki and in agreement with the ethical guidelines of the Japan Society of Obstetrics and Gynecology.

Human Neurosphere Culture

Human neural precursor cell cultures were established using the neurosphere method (14). The cells used had been cultured for more than 1 year. Cells were cultured in Dulbecco's modified Eagle's medium (DMEM)/F12 serum-free medium complemented with B27 supplement (Gibco, Grand Island, NY), recombinant human epidermal growth factor (20 ng/ml; R&D, Minneapolis, MN), recombinant human basic fibroblast growth factor (20 ng/ml; Genzyme TECHINE, Minneapolis, MN), leukemia inhibiting factor (Chemicon, Temecula, CA), and heparin (Sigma, St. Louis, MO). For differentiation, the cells were dissociated with 0.05% trypsin (Gibco) for 20 minutes at 37°C and plated on polyornithine- and laminin-coated glass coverslips (Sigma), followed by incubation with DMEM/F12 medium with either B27 supplement or 10% fetal bovine serum for 6 days.

Mouse Neurosphere Culture

Murine neural precursor cells were established from E12.5 and E14.5 ICR embryos using the neurosphere method (15). Briefly, embryos were removed from the uterus of timed pregnant mice and placed in a Petri dish containing Hanks' balanced salt solution (Gibco). The mouse telencephalon was freed from meninges, and the cells were dissociated by mechanical trituration with a fine narrowed Pasteur pipette. After centrifugation at 800 rpm for 3 minutes, the cells were resuspended in the same culture medium used for human neurosphere culture (but without leukemia inhibiting factor and heparin) and cultured in a humidified atmosphere of 5% CO_2 incubator at 37°C. Half of the

medium was changed every 3 days. Primary neurospheres were cultivated for 6 to 10 days before harvest.

For differentiation, 5 to 10 neurospheres were attached onto polyornithine- and laminin-coated glass coverslips (14-mm diameter) in a 24-well plate (Nunc, Roskilde, Denmark) and cultured up to 14 days with DMEM/F12 medium containing either B27 supplement or 10% fetal bovine serum.

Anti-SMARCAL1 Antibody Production

An anti-SMARCAL1 antiserum was generated as previously described (16). The antiserum identifies a specific antigen that is not present in patients with biallelic nonsense mutations of SMARCAL1. It recognizes a specific band of the appropriate molecular weight on Western blots of human tissue extracts.

Western Blotting

The fetal human brain samples were removed at autopsy, snap-frozen in liquid nitrogen, and stored at −80°C; the adult human brain samples were purchased from BD Biosciences (Franklin Lakes, NJ). Tissues were homogenized in 2× sodium dodecyl sulfate (SDS) sample buffer (Invitrogen, Carlsbad, CA) and boiled for 5 minutes. Protein (10 μg) was loaded into each well, fractionated on a 7% SDS-polyacrylamide gel electrophoresis gel, and transferred to a polyvinylidene fluoride membrane (Invitrogen). After blocking with phosphate-buffered saline (PBS) containing 0.2% I-Block (Applied Biosystems, Foster City, CA) for 1 hour at room temperature (RT), a 1:5000 dilution of the anti-SMARCAL1 rabbit polyclonal antibody and a 1:5000 dilution of anti-glyceraldehyde 3-phosphate dehydrogenase mouse monoclonal antibody (MAB374; Chemicon) were incubated with the membrane for 1 hour at RT. After incubation with the primary antibodies, the Western blots were washed with blocking buffer 3 times for 10 minutes each at RT and then incubated with alkaline phosphatase-conjugated secondary antibodies (anti-rabbit immunoglobulin (Ig)G and anti-mouse IgG: A2556 and A3562, respectively; Sigma) for 30 minutes at RT. The blots were then washed 3 times for 10 minutes each at RT. The bound antibody was detected by chemiluminescence using CDP-Star (Applied Biosystems) according to the manufacturer's specifications.

Immunohistochemistry

Human and mouse brains were fixed by immersion in 10% buffered formalin or 4% paraformaldehyde (PFA) in PBS. The brain tissue was processed, embedded in paraffin, and cut into 8-μm sections according to standard protocols (17). Immunohistochemistry was done as previously described (16). We used the following primary antibodies: polyclonal rabbit anti-human SMARCAL1 (BCM312), diluted 1:200; monoclonal mouse anti-rat Musashi1 (14H1 [18]), diluted 1:500; anti-human Hu (18), diluted 1:1000; and a polyclonal anti-glial fibrillary acidic protein (GFAP; Dako, Carpinteria, CA), diluted 1:1000.

Immunofluorescence

To determine the cell types in which SMARCAL1 was expressed in the human and the mouse brain, we performed double immunofluorescence using a 27–GW human brain and mouse brains ranging in age from E8.5 to adult. The brains were fixed in 4% PFA for 48 hours, immersed in 30% sucrose for 48 hours, and then frozen in optimal cutting temparature-embedding medium on dry ice. After cutting 8- to 20-μm-thick sections using a cryostat, the tissue sections were placed on Superfrost plus microslides (VWR International, West Chester, PA) and incubated with the primary antibodies in 10% normal horse serum for 2 hours at RT or overnight at 4°C. The sections were then rinsed with PBS with 0.02% Tween. For visualization, we used the Alexa 568-conjugated secondary antibodies anti-rat IgG, anti-rabbit IgG, and anti-human IgG, and the Alexa 488-conjugated secondary antibodies anti-rat IgG, anti-rabbit IgG, and anti-human IgG (Molecular Probes, Eugene, OR). After incubation with the secondary antibodies for 30 minutes at RT, the tissue sections were rinsed 4 times with PBS with 0.02% Tween and mounted in Vectashield (Vector Laboratories, Burlingame, CA).

Human and mouse neurospheres and single neural precursor cells grown on coverslips were fixed in 4% PFA in PBS for 15 minutes at RT, washed 3 times with PBS, permeabilized with 0.3% Triton X-100 in PBS for 5 minutes, washed 3 times with PBS, and blocked with 5% horse serum in 1% casein (PIERCE, Rockford, IL) for 30 minutes at RT. Primary antibodies were diluted in 10% horse serum in PBS and incubated with the fixed cells overnight at 4°C. After washing in PBS, secondary antibodies diluted in PBS were incubated with the fixed cells for 30 minutes at RT and mounted in Vectashield (Vector Laboratories). Images were acquired using a Zeiss Axiovert 200 microscope (Jena, Germany), a Zeiss AxioCamHR (bright-field) or a Zeiss AxioCamMR camera (fluorescence), and the Zeiss AxioVision imaging system. Confocal images were acquired as image stacks of separate channels with a Zeiss LSM 510 microscope and combined and visualized with Zeiss LSM Image Browser v3.2.

Reverse-Transcriptase-Polymerase Chain Reaction

Total RNA was extracted from 2 independent human neural stem cell cultures using the RNeasy kit (Qiagen). The RNA was reverse transcribed into cDNA using random primers and RNase H-MMLV reverse transcriptase (Stratagene). Primers specific to the human SMARCAL1 cDNA were designed and used for polymerase chain reaction (PCR) amplification (30 cycles of 94°C for 30 seconds, 55°C for 30 seconds, and 72°C for 1 minute). Amplification of actin cDNAs was used as a reference control. The primer pairs used were 5′-CAGGACCTTATTGCGCTTTT-3′ and 5′-CGGGCAGTCCTACTGTTTTT-3′ for human SMARCAL1 PCR and 5′-GCTCACCATGGATGATGATATCGC-3′ and 5′-GGAGGAGCAATGATCTTGATCTTC-3′ for actin. The PCR products were run on a 2% agarose gel and detected by ethidium bromide.

Northern Blot Analysis

Human tissue Northern blots were purchased from Clontech (Mountain View, CA) and hybridized according to the manufacturer's instructions. Mouse brains (E14.5 adult)

or heads (E9.5–E12.5) were dissected and snap-frozen in liquid nitrogen. Total RNA was prepared using the Ambion total RNA kit (Ambion, Austin, TX). Total RNA (20 μg) of each sample was loaded onto 1% agarose-formaldehyde gel and transferred to a nylon membrane (Ambion) overnight by capillary transfer using 20× sodium chloride-sodium citrate (SSC). After prehybridization in hybridization buffer (15% formamide, 40 mmol/L of $NaPO_4$, pH 7.2, 10 mmol/L of EDTA, 7% SDS, 2% bovine serum albumin), the filters were hybridized with ^{32}P-labeled cDNA probes in fresh buffer at 65°C overnight. DNA probes for Northern hybridization were synthesized from the human or the mouse 5′-untranslated region of the SMARCAL1/Smarcal1 cDNA using a random-prime labeling system (Amersham, Piscataway, NJ). Hybridized membranes were washed in buffer (40 mmol/L of $NaPO_4$, 1 mmol/L of EDTA, 1% SDS) 3 times for 30 minutes each at 65°C and exposed to film. As a control for the amount of RNA loaded in each lane, the probe was stripped from the membrane with 10 mmol/L of Tris-HCl, 1 mmol/L of EDTA, 0.1% SDS containing buffer at 100°C, and the membrane was rehybridized with a glyceraldehyde 3-phosphate dehydrogenase probe.

In Situ Hybridization

Digoxigenin-labeled mouse Smarcal1 antisense and sense riboprobes were synthesized using an in vitro transcription kit (Roche, Indianapolis, IN) according the instructions. The fresh brain sections were sectioned at 10 μm. Sections were fixed in 4% PFA for 20 minutes and washed twice in 1× PBS, treated with 0.1 N of HCl for 20 minutes, digested with proteinase K in 1× TE at 37°C for 10 minutes, washed once in deionized water, postfixed with 4% PFA for 20 minutes, then incubated in 0.25% acetic anhydride/0.1 mol/L of triethanolamine (pH 8.0) for 10 minutes. After a brief wash with 2× SSC, the sections were prehybridized for 1 hour at 55°C in the hybridization buffer containing 50% deionized formamide, 0.2% SDS, 0.75 mol/L of NaCl, 25 mmol/L of piperazine diethanesulfonic acid, 25 mmol/L of Tris-HCl and EDTA, 1× Denhardt and 50 μg/ml of salmon sperm DNA, and hybridized in the same buffer containing 1 μg/ml of either antisense or sense Smarcal1 probe at 55°C overnight. After hybridization, the sections were rinsed briefly in 4× SSC at 55°C 5 times for each 5 minutes and 2× SSC for 30 minutes at 55°C. After a 10-minute wash with RNase buffer containing 10 mmol/L of Tris-HCl and 0.5 mol/L of NaCl, the unbound RNA probes were digested with 20 μg/ml of RNase A in the same buffer for 30 minutes at 37°C. The sections were then washed 2 times in 0.1× SSC for 15 minutes at RT. After several rinses in Tris-buffered saline (0.15 mol/L of NaCl, 0.1 mol/L of Tris, pH 7.5), the sections were incubated in 0.5% blocking solution (Roche) for 30 minutes at RT, followed by incubation for 2 hours with alkaline phosphatase-conjugated sheep anti-digoxigenin antibody (1:1000; Roche) at RT. After several washes with 50 mmol/L of $MgCl_2$ in Tris-buffered saline, pH 9.5, the phosphatase reaction was performed using nitroblue tetrazolium-5-bromo-4-chloro-3-indolylphosphate as substrates. The color reaction was developed in the dark until satisfying results were obtained.

RESULTS

Neurodevelopment of SIOD Patients

To ascertain whether SIOD patients have neurologic abnormalities, we sent questionnaires to the physicians of 38 SIOD patients with identified *SMARCAL1* mutations and received 33 responses (Table 1). Half of the patients had a head circumference less than the third percentile. We did not detect a significant correlation of head circumference with disease severity as scored using our previously defined scale (19) or with age at death (Figs. 1A, B). Stature was neither predictive of head circumference nor was the head circumference always disproportionately larger or smaller (Fig. 1C); nearly half had disproportionately large or small heads, and of these, half were larger and half were smaller. To date, imaging studies have not identified structural abnormalities indicating a cause of abnormal head growth (16).

We also compared head circumference to the different patient mutations to determine whether the *SMARCAL1* mutations were predictive of head circumference. Among patients with a sequence variant encoding a nonsense, frameshift, or deletion mutation on both alleles, 60% had a head circumference less than the third percentile; among patients with a sequence variant encoding a nonsense, frameshift, or deletion mutation on 1 allele and a sequence variant encoding a missense mutation on the other allele, 57% had a head circumference less than the third percentile; and among patients with sequence variants encoding missense mutations on both alleles, 44% had a head circumference less than the third percentile (Fig. 1D). These observations suggest a trend toward preserved brain growth in the background of biallelic missense mutations, but the number of patients is too small for this to be statistically significant.

As assessed by their primary care physicians, 5 of the 33 patients had mild delay of 1 or more developmental parameter; only 1 patient (Patient 57), who had a stroke at 4 years of age, had warranted formal developmental testing and required intervention services (20). Of the 26 patients who attended school, 22 had normal school performance. All patients with a disproportionately large head circumference (Patients 16, 28, 30, 33a, 39, 44, 47, and 51) had normal development, whereas 1 (Patient 27) of 6 patients (Patients 23, 27, 45, 49, 60, and 71) with a disproportionately small head circumference did not. The mutation type was not predictive of a disproportionately small or large head size or of the developmental pattern. Several patients had electroencephalographic (EEG) abnormalities such as excessive background slowing and foci of rhythmic and arrhythmic slowing, but only 2 patients manifested clinical seizures prior to the onset of cerebral ischemia (Table 1).

SMARCAL1 Expression During Human and Mouse CNS Development

The findings of frequent microcephaly and EEG abnormalities among SIOD patients prior to their manifestation of cerebral ischemia suggested that SMARCAL1 may play an autonomous role in neurodevelopment. Therefore, we

TABLE 1. Clinical Features of 33 Patients with SIOD and *SMARCAL1* Mutations

Patient (mutation [19])	OFC Percentile	Height Percentile	Disease Severity Score* (maximum = 5)	Delay	Physician's Assessment of Developmental Delay				School Performance	Seizure	EEG Abnormality	Memory Problem	Mood Problem	Age, years	
					Motor	Language	Social	Intellect						Death	Current
Survival < 20 years															
33a (c.1146_1147delAA+ c.1147+ 1_2delGT, c.1097-2A9G)	3–10	<3	3	No					N/A			UA	UA	2.75	
50 (c.2542G>T)	<3	<3	3	No					Normal	Yes§	Yes	No	No	8	
53 (c.2291G>A, c.2542G>T)	50	50	3	No					Normal			UA	UA	13.5	
8 (c.1190delT)	<3	<3	4	No					N/A	UA	UA	UA	UA	5.7	
23 (c.2542G>T)	<3	3–10	4	No					N/A‡			No	No	10.25	
28 (c.1702delG)	50	3–10	4	No					Normal	No	No	No	No	12	
31 (Del ex1-4)	<3	<3	4	No					Normal			No	No	14	
35 (c.1736C>T, c.2321C>A)	<3†	<3	4	No					Normal			No	No	8	
47 (c.2459G>A)	25–50	<3	4	No					Normal			No	No		16.6
48 (c.1939A>C)	<3	3	4	Yes	Mild delay	Mild delay	Mild delay	Mild delay	N/A	No	No	No	No	6	
49 (c.1920_1921insG)	<3	10	4	No					Normal			UA	UA	4.8	
60 (c.2542G>T)	<3	25	4	No					Normal			No	No	13.6	
61 (c.1146_1147delAA+ c.1147+1_2delGT)	UA	<3	4	No					N/A			No	No	5	
66 (c.1933 C>T)	<3†	<3§	4	No					Normal			No	No	13	
68 (c.1940 A>C, c.2462 T>G)	3–10	3–10	4	No					Normal			Yes	Yes	7.1	
72 (c.836T>C, c.1136A>C)	<3	<3	4	No					Normal		Yes	Yes	Yes	9.6	
74 (c.1736C>T)	10–25	10–25	4	No					N/A			No	No		7.5
24 (Del ex1-4)	<3†	<3†	5	Yes		Mild delay	Mild delay	Mild delay	Mild delay	Yes‖	Yes	No	No	9	
25 (c.49C>T, c.100C>T)	50†	UA	5	No					Normal	Yes‖		No	No	10.1	
29 (c. 1934delG, c.862+1G>T)	<3	<3	5	Yes					N/A			UA	UA	4	
30 (c.1132G>T)	10–25	<3	5	No					Normal			No	No	10	
38 (c.1096+1G>A)	<3	<3	5	Yes	Mild delay		Mild delay		Normal	No	Yes	No	No	10.75	
39 (c.1402G>C, c.2114C>T)	10–25†	10	5	No					Normal	Yes¶	Yes	No	Yes	15	
44 (c.1191delG, c.2321C>A)	3–10	3	5	No					Normal			UA	UA	11.9	
51 (c.2542G>T, c.2459G>A)	25	<3	5	No					Normal	No	Yes	No	No		12
71 (c.836T>C, c.1000C>T)	<3	3–10	5	No					Normal			Yes	No		10.8
Survival ≥ 20 years															
65a (c.836T>C, c.2542G>T)	90	75	1	No					Normal			No	No		26.9
27 (c.1940A>C)	<3	3–10	2	Yes				Mild delay	Mild delay			No	No	25.6	
45 (c.1874C>G, c.2459G>A)	<3	25	2	No					Normal			UA	UA		28.1
65b (c.836T>C, c.2542G>T)	25	25	3	No					Normal			Yes	No		24
16 (c.1643T>A, c.1933C>T)	50†	<3	3	No					Normal			No	No		32
57 (c.955 C>T)	3–10	3–10	4	Yes	Mild delay	Moderate delay	Mild delay	Mild delay	Moderate delay	Yes‖	Yes	Yes	Yes		25.9
84 (c.1248_1249insC, c.2104T>G)	<3†	<3	5	No					Normal			No	No	23	

*, Point system reflecting the severity of symptoms associated with SIOD: linear growth failure before 10 years of age received 1 point; renal failure received 1 point; lymphopenia received 1 point; recurrent infections received 1 point; cerebral ischemia received 1 point (19).

†, Percentile at first clinic visit with reporting physician. For all others, the percentile at birth is given.

‡, Patient had a severe stroke prior to beginning school and was never able to attend mainstream schools.

§, One generalized seizure at 3 years, apparently unrelated to cerebral ischemic events.

‖, Seizures started after the onset of cerebral ischemic events.

¶, One generalized seizure at 13 years, apparently unrelated to cerebral ischemic events.

N/A, not applicable; OFC, occipital-frontal circumference; SIOD, Schimke immuno-osseous dysplasia; UA, unavailable.

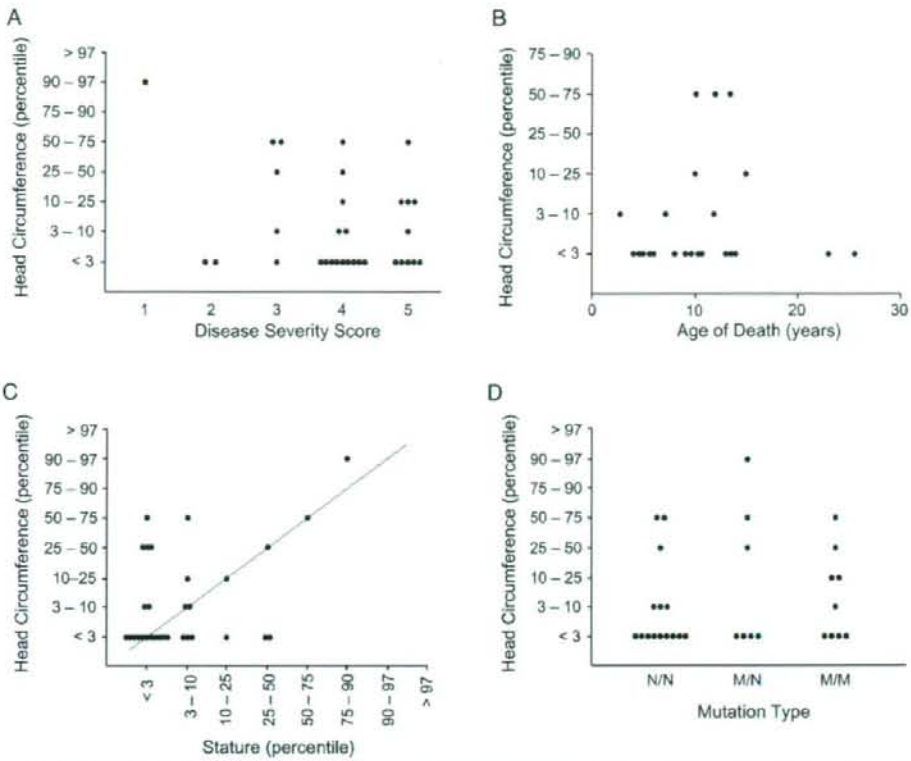

FIGURE 1. Analysis of SIOD patient head circumferences. **(A)** Comparison of head circumference to disease severity. **(B)** Comparison of head circumference to age of death. **(C)** Comparison of head circumference to stature. **(D)** Comparison of head circumference to predicted SMARCAL1 mutation. M, a sequence variant encoding a missense mutation; N, a sequence variant encoding a nonsense, frameshift, or deletion mutation.

hypothesized that SMARCAL1 would be expressed in the mouse and human nervous system and profiled its expression in the developing and mature mouse and human CNS. In the mammalian brain, the Layer I Cajal-Retzius neurons are the first neurons to mature. Other cortical neurons are generated from neural stem cells in the neuroectoderm surrounding the ventricles, that is, the ventricular zone (VZ) and subventricular zone (SVZ), and migrate to form the cortex. Astrocytes and oligodendrocytes also arise from the stem cells in the VZ and SVZ. As the brain matures, the VZ and SVZ retain a small number of neural precursors (21).

As each cell type migrates away from the VZ and SVZ, it differentiates, and this maturation can be detected by expression of specific proteins. The markers followed were as follows: 1) Musashi1 and Nestin, which are markers of neural precursors, immature neurons, and immature astrocytes (18, 22–24); 2) Hu, which is a marker of postmitotic immature and mature neurons (25); 3) GFAP, which is a marker of immature and mature astrocytes (26); and 4) O4 and 2′,3′-cyclic-nucleotide 3′-phosphodiesterase, which are markers of immature and mature oligodendroglia (27, 28).

As assessed by Northern (Fig. 2A) and Western (Fig. 2B) blots, in situ hybridization (Figs. 2C–L), and immunohistochemistry (Figs. 2M–P), we demonstrated that Smarcal1 is expressed in the developing and mature mouse brain. In the embryo, Smarcal1 was strongly expressed in the VZ, SVZ, intermediate zone, and cortical plate (data not shown). In postnatal brains, we observed Smarcal1 expression in the VZ and SVZ, as well as in cortical, cerebellar, spinal, and peripheral neurons (Figs. 2C–P).

By immunofluorescent colocalization studies in the adult mouse brain, we observed cortical colocalization of Smarcal1 with the neuronal marker Hu in postmitotic neurons (Figs. 3A–D), but not with GFAP in mature astrocytes (Figs. 3E–H). In the ependyma and the VZ and SVZ, Smarcal1 colocalized with the precursor cell marker Musashi1 (Figs. 3I–L) and with GFAP in a few SVZ cells (data not shown). We also confirmed expression of Smarcal1 in cultured mouse neural precursors by immunofluorescence (Figs. 3M–R) and Western blot (Fig. 3S) analyses of mouse neurospheres.

We next determined the cell type-specific temporal and spatial distribution of SMARCAL1 in the human brain by Western blot analysis (Figs. 4A, B) and by immunohistochemistry (Figs. 4C–I). We performed immunohistochemistry on 40 human brains ranging in age from 10 GW to 61

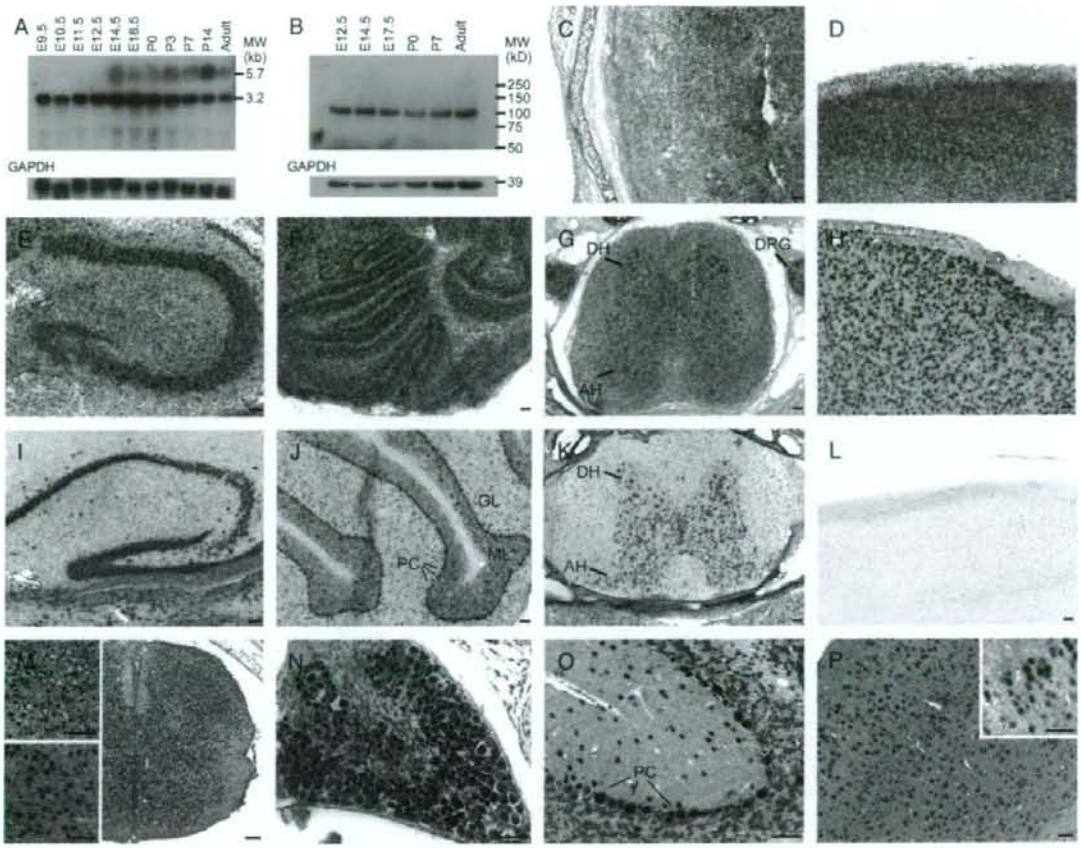

FIGURE 2. Northern blot, Western blot, in situ hybridization, and immunohistochemical analyses of Smarcal1 expression in the murine brain. **(A)** Northern analysis for Smarcal1 mRNA expression in the developing mouse brain. Each lane contained 20 μg of total RNA. For samples E9.5 to E12.5, the RNA was derived from whole head extracts. For samples E14.5 to adult, the RNA was derived from isolated brains. **(B)** Western analysis for Smarcal1 expression in protein extracts from the whole mouse brains from developmental stages E12.5, E14.5, E17.5, P0, P7, and adult. Panel shows a single Smarcal1 protein band despite detection of 2 mRNA bands on the Northern shown in **(A)**. The membrane was concurrently probed for glyceraldehyde 3-phosphate dehydrogenase expression to control for protein integrity and loading. **(C–L)** In situ hybridization detection of Smarcal1 expression in the P0 cerebrum **(C)**, in the P7 cortex **(D)**, P7 hippocampus **(E)**, P7 cerebellum **(F)**, P7 spinal cord, and P7 dorsal root ganglia **(G)**, and in the adult cortex **(H)**, adult hippocampus **(I)**, adult cerebellum **(J)**, and adult spinal cord **(K)**. **(L)** Panel shows hybridization of the sense control probe to a serial section of adult cortex. **(M–P)** Immunohistochemical detection of Smarcal1 protein expression in the adult spinal cord **(M)**, dorsal root ganglion **(N)**, cerebellum **(O)**, and cortex **(P)**. The upper inset in **(M)** is a higher magnification of the dorsal horn, and the lower inset is a higher magnification of the anterior horn. The inset in **(P)** is a higher magnification of cortical Layer II. Bar = 50 μm. AH, anterior horn; DH, dorsal horn; DRG, dorsal root ganglion; E, embryonic day; GAPDH, glyceraldehyde 3-phosphate dehydrogenase; GL, granular layer; ML, molecular layer; P, postnatal day; PC, Purkinje cell.

years (23 prenatal and 17 postnatal). In prenatal brains, there was strong nuclear expression of SMARCAL1 in most cells of the immature cortex, in some cells within VZ and SVZ, and along the migratory pathway from the VZ/SVZ to the cortex (Fig. 4C).

Among the 17 postnatal brains (newborn to 61 years old), SMARCAL1 was expressed in the nuclei of a subset of cells in the SVZ and in a subset of cortical neurons (Figs. 4D–F). Expression in cells in the white matter decreased with age (data not shown). SMARCAL1 continued to be expressed predominantly in the nuclei of cortical neurons in the postnatal brains (Figs. 4D–F), although at a lower staining intensity than in the fetal brain. Expression in human neural precursors was confirmed by immunofluorescent (Fig. 4J–L) and reverse-transcriptase-PCR (Fig. 4M) analyses of cultured human neurospheres.

Neuropathology of SIOD Patients

The clinical observations of frequent small head circumference and EEG abnormalities in SIOD patients and the

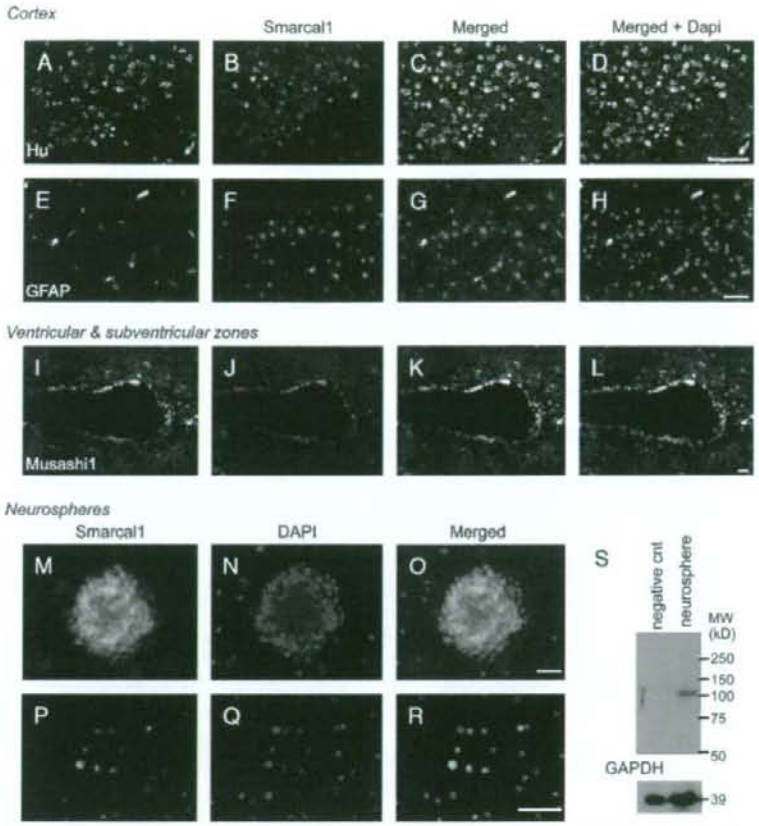

FIGURE 3. Immunofluorescent characterization of Smarcal1 expression in an adult mouse brain. Smarcal1 colocalizes with Hu **(A–D)** but not with glial fibrillary acidic protein **(E–H)** in the cortex, and with Musashi1 in the ventricular zone and subventricular zone **(I–L)**. As detected by immunofluorescence **(M–R)** and Western blot **(S)**, Smarcal1 is also expressed in cultured neurospheres **(M–O)** and in the individual cells dissociated from the neurospheres **(P–R)**. The negative control for the Western blot is an extract from lymphoblastoid cells from a patient homozygous for deletion of the *SMARCAL1* gene promoter and first 4 exons. Bar = 50 μm. cnt, control; GAPDH, glyceraldehyde 3-phosphate dehydrogenase.

expression of SMARCAL1 during brain development suggest that deficiency of SMARCAL1 may cause defective neurodevelopment. To investigate this possibility, we examined available microscopic sections of brain tissue on Patient SD60, who died of cardiopulmonary arrest at the age of 13 years (10), and Patient SD 84, who died of pulmonary hypertension and right heart failure at the age of 23 years (21). Both had had a head circumference of less than the third percentile and normal language, social, motor, and cognitive development. They had excelled academically, as is usual for SIOD patients prior to the onset of cerebral ischemic attacks, and they did not have a seizure disorder. The neuropathologic examination in these cases is regrettably incomplete. Vascular pathology was observed and was previously reported based on our initial observations of several microscopic slides that were available from autopsy material (10). Upon request, additional microscopic slides and some paraffin blocks were kindly sent to us by referring institutions; however, not all regions were sampled or identified. Despite these limitations, we studied the available materials and report our interpretations for comparison to more complete analyses.

Because of the limited samples available, the following observations cannot be considered conclusive or complete. Rather, they are to serve as a basis for future studies. According to the autopsy reports, the brains of Patients SD60 and SD84 weighed less than normal and had areas of infarction and ischemia (Table 2). Despite normal CNS function and antemortem brain magnetic resonance imaging, the nonischemic areas of both brains had very subtle, but consistent, histologic abnormalities. In several focal regions of cerebellar folia, the Purkinje cells (as defined by serial sectioning) seemed to be poorly aligned (Supplemental Fig. 2A); however, because of incomplete materials, the vermis, which has been reported as abnormal by magnetic resonance imaging in some SIOD patients (29), could not be assessed. In the cerebral cortex and the subcortical white matter, focal structural anomalies were observed in 50% of the available cortical sections. The microscopic

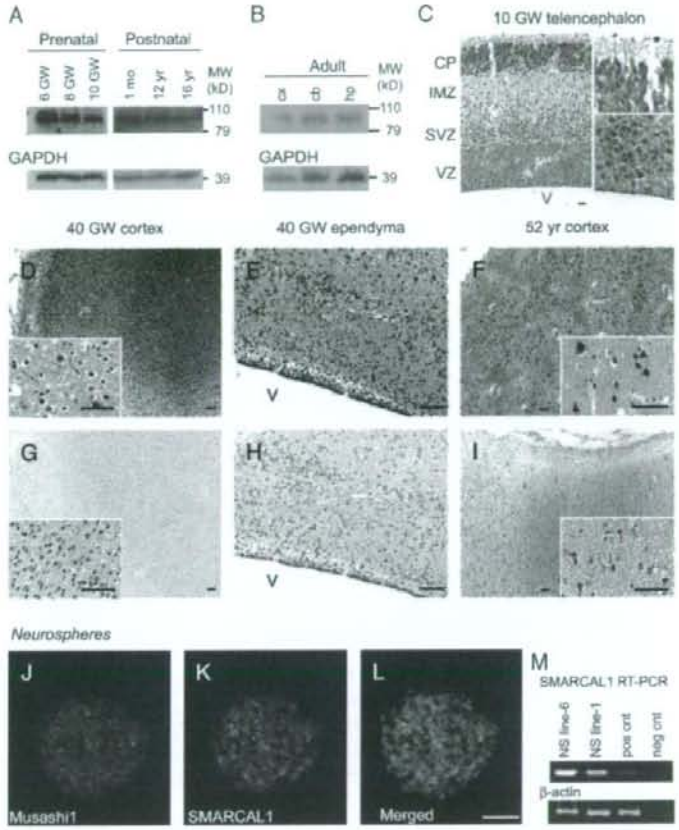

FIGURE 4. Western blot and immunohistochemical analyses of SMARCAL1 protein expression in the human brain. **(A)** Western analysis for SMARCAL1 expression in protein extracts from whole human brain at 6, 8, and 10 gestational weeks (GW); the brain is predominantly neural precursors at 6 weeks of gestation. The membrane was concurrently probed for glyceraldehyde-3-phosphate dehydrogenase (GAPDH) expression to control for protein integrity and loading. **(B)** Western analysis for SMARCAL1 expression in protein extracts from the cortex (cx), cerebellum (cb), and hippocampus (hp) of the adult human brain. The membrane was concurrently probed for GAPDH expression to control for protein integrity and loading. **(C)** SMARCAL1 expression in the cerebrum of a human 10-GW brain. Cells in the ventricular zone (VZ), subventricular zone (SVZ), IMZ, and the CP express SMARCAL1. Higher-magnification image of SMARCAL1 expression in the CP of the human 10-GW brain (upper inset). Higher-magnification image of SMARCAL1 expression in the VZ and SVZ of the human 10-GW brain (lower inset). **(D, E)** Expression of SMARCAL1 in the cortex and ependyma of a 40-GW brain. The inset **(D)** shows SMARCAL1 expression in cortical Layer II. **(F)** Expression of SMARCAL1 in adult cortical neurons. The inset shows SMARCAL1 expression in cortical Layer II. **(G–I)** Serial sections treated with preimmune serum. As detected by immunofluorescence **(J–L)** and reverse-transcriptase-polymerase chain reaction **(M)**, SMARCAL1 is also expressed in cultured neurospheres. Bar = 50 μm. cnt, control; CP, cortical plate; IMZ, intermediate zone; V, ventricle.

malformations included subcortical "heterotopias," some of which were verified by serial sectioning to be separate from the cortex and not related to tangential sectioning (Supplemental Fig. 2B). Upon serial sectioning, some of the heterotopias (Supplemental Fig. 2B; marked with a star) represented an extension of the "expanded cortex" as described in the succeeding sentences. Within these areas, no organization of neurons could be discerned. There were also isolated sections of expanded cortex. For example, the cortical thickness in temporal cortex of SD84 ranged from 2.0 to 6.0 mm, whereas in an age-matched control, the same regions measured 1.5 to 4.5 mm. In the "thicker" regions of cortex, there were usually several other associated findings. There was a loss of a well-defined Layer II in each section examined (Supplemental Fig. 2C) as defined by calbindin immunoreactivity, which is normally present in only Layer II neurons (control frontal cortex; Supplemental Fig. 2D). There was poor definition of the cortical gray-white matter junction similar to that observed in cortical dysplasia. In addition, near the expanded cortex, serial sections frequently revealed a failure of separation of gyri and aberrant definition of sulci (data not shown). Importantly, the malformations were

TABLE 2. Summary of Brain Pathologic Findings in SIOD Patients SD60 and SD84

	SIOD Patient	
	SD60	**SD84**
Gross pathology		
Brain weight	1,100 g (normal, 1,300 g)	1,020 g (normal, 1,300–1,400 g)
Blood vessels*	Abnormal	Abnormal
Cerebrum	Normal gross structure, diffuse ischemic changes	Normal gross structure, recent and old focal infarcts
Cerebellum	Normal gross appearance, possible focal Purkinje cell crowding	Normal gross appearance, possible focal Purkinje cell crowding
Brainstem	Normal	Normal
Cortical pathology		
Focal cortical expansion	4/9†	10/24†
Subcortical heterotopia	1/9†	4/24†
Incomplete sulcation	3/9†	5/24†
Displaced Layer II	2/2‡	3/3‡

*, The blood vessel pathology is described in Reference 10.
†, The denominator is the number of cortical sections available, and the numerator is the number of these sections with the observed alteration.
‡, The denominator is the number of cortical sections stained with anti-calbindin, and the numerator is the number of these sections with the abnormal localization of calbindin-positive neurons.
SIOD, Schimke immuno-osseous dysplasia.

microscopic and required serial sectioning to assess their positions within the cortex. Probably only a powerful and detailed imaging system could have identified them in the living patient.

Because of the role of SMARCAL1 in cell proliferation and its presence in neural precursor cells (and because of the findings in the SIOD cases), we questioned whether neural precursor cells can be identified in subventricular regions in the brain tissue samples. Using the markers Mushashi-1 and Nestin (30), we detected neural precursor cells, indicating that there was not a complete absence of these neural precursor cells in these small brains (Supplemental Figs. 3A–L). There were, however, fewer of them than in the control brain sample (Supplemental Fig. 3P).

Knockdown Studies in Mouse Neurospheres

Based on the suggestion that deficiency of SMARCAL1 contributes to a reduced number of precursors, we performed siRNA knockdown of Smarcal1 in mouse neurospheres. The results indicated that the neurospheres grow less well when they were made deficient in Smarcal1 (Supplemental Figs. 3Q–U). Using 2 different siRNA oligonucleotides for Smarcal1 neurospheres derived from ICR and 129 SvEv mice, 3 independent experiments for each condition showed 53% to 67% transfection efficiency and, as measured by Western blot, a 40% to 50% knockdown of SMARCAL1 protein 4 days after transfection (Supplemental Fig. 3V). Four days after transfection with the Smarcal1 siRNA, the number and radii of neurospheres as well as the number of cells per neurosphere were significantly reduced ($p < 0.001$), whereas cells transfected with the control siRNA were unaffected (Supplemental Figs. 3Q–U). Therefore, although deficiency for SMARCAL1 does not cause a complete loss of neural precursors, it may be one factor contributing to the small brain size in these patients. These results require confirmation both when there are additional studies on SIOD patient tissues and when *Smarcal1* knockout mice become available.

DISCUSSION

SMARCAL1 is a unique member of the SNF2 family of chromatin remodeling proteins that have DNA-dependent adenosine triphosphatase activity (12, 31). We recently determined that mutations of SMARCAL1 cause SIOD (9). In this report, we show for the first time that 1) there is expression of SMARCAL1 in CNS neurons and neural precursors in both humans and mice; 2) SIOD patients often have a reduced head circumference (microcephaly); and 3) autopsy observations of 2 male SIOD patients identify subtle histologic features suggestive of perturbed neuron-glial migration that warrant confirmation and detailed examination in future autopsy studies of SIOD.

The microcephaly is consistent with our previous hypothesis that SMARCAL1 expression facilitates cellular proliferation (9, 10, 19). The head circumference measurements were obtained at birth or prior to the onset of cerebral ischemia, which contributes to reduced brain weight and the acquired cerebellar atrophy reported in some SIOD patients (29). Surprisingly, the microcephaly did not correlate with other clinical features, and despite microcephaly and the subtle histologic features suggestive of perturbed neuron-glial migration, most SIOD patients had generally normal social, language, motor, and cognitive development, and very few had seizures (Table 1). These observations suggest that SMARCAL1 participates in the modulation of both neural proliferation and differentiation but that the morphologic abnormalities that result from deficiency of SMARCAL1 rarely cause serious neurophysiologic dysfunction or developmental deficits. Examination of the brains from SIOD patients who manifest abnormal development or seizures would, however, clarify the range of CNS abnormalities associated with SMARCAL1 deficiency.

The lack of overt functional CNS deficits in most SIOD patients contrasts with the severe neurologic deficits observed with deficiency of the SNF2 factor α-thalassemia mental retardation, X-linked syndrome (32). Individuals with primary microcephaly may, however, have minimal neurologic problems (33–35). Unlike many other skeletal dysplasias and genetic disorders of generalized growth, the relationship between stature and head circumference is not uniform in SIOD. This suggests that loss of SMARCAL1 function is not sufficient for the development of microcephaly, and that stochastic, epigenetic, environmental, or other genetic factors might also contribute to the microcephaly in SIOD patients.

Poor brain growth can result from a reduction in cell number or size but generally has been ascribed to a reduction in cell number (36). Such a reduction can arise either from reduced proliferation or from increased death of glia and/or neurons (37). Based on the spatio-temporal expression of SMARCAL1/Smarcal1 in the human brain, SMARCAL1 deficiency might affect neural precursor viability from early in embryogenesis to postnatal life, thereby contributing to the decreased mean prenatal and postnatal head circumferences observed in many of the patients with SIOD. Moreover, the early-onset cognitive impairment that we have observed in some adult SIOD patients might be attributable to a failure of ongoing neurogenesis in addition to the cerebrovascular disease that results in stroke-like episodes (10, 29, 38, 39).

In addition to the modulation of numbers of neural precursor cells, our findings also implicate SMARCAL1 in the regulation of neuronal migration and cortical differentiation. The presence of microscopic periventricular heterotopia, cortical microdysgenesis, and aberrant gyration seen in both autopsy cases have been observed in other disorders of neural migration and cortical patterning (40). Cortical microdysgenesis has been associated with infantile spasms (41), primary generalized epilepsy (42), partial epilepsy (43), dyslexia (44, 45), congenital mental retardation (46), and autism-like disorders (46). Although neither of the autopsy cases we studied was associated with these disorders, histories of the clinical cohort did reveal some of these conditions: 2 SIOD patients had seizures, 7 had EEG changes, and there was mild mental delay in 7. These clinical features in SIOD patients warrant careful examination for evidence of histologic correlates that may suggest perturbed neuron-glial migration. It might also be worth considering whether SIOD patients, who have generally intractable migraine-like headaches, might also be manifesting a partial seizure disorder (16, 47).

The histologic features suggestive of perturbed neuron-glial migration identified would arise from a disturbance in the later stages of radial neuronal migration and cortical organization, whereas heterotopias would arise as a disturbance of the earlier stages of radial neuronal migration. The molecular basis of the cortical microdysgenesis in neurologic disorders is undefined, although some have suggested aberrant secretion of reelin by Cajal-Retzius neurons (48). We found expression of SMARCAL1 in the migrating neuronal precursors, cortical neurons, and in the Cajal-Retzius neurons, but not in cortical oligodendrocytes or astrocytes (Fig. 5). Based on our prior studies suggesting a cell-autonomous function for SMARCAL1 (10, 49, 50), we

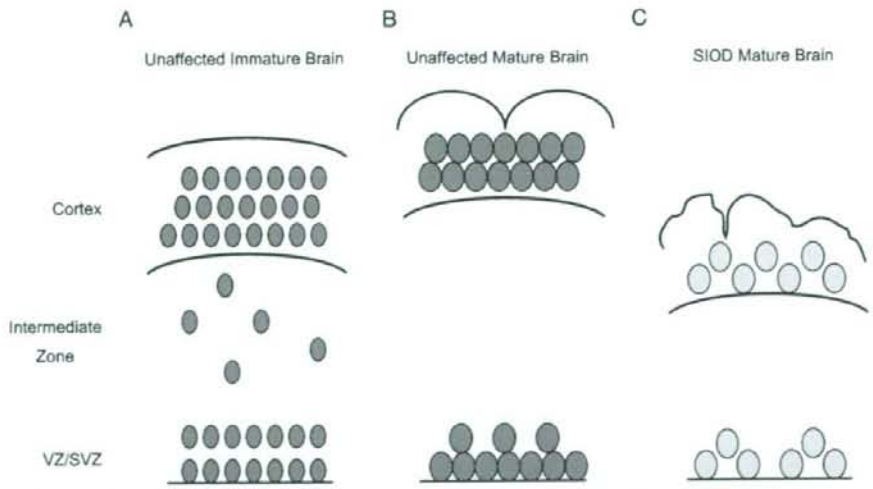

FIGURE 5. Schematic of SMARCAL1/Smarcal1 expression during brain development. **(A)** In normal developing brain, SMARCAL1 is present in cells of neuronal lineage, including neural precursor cells, migrating immature neurons, and postmigrating neurons in cortex. **(B)** SMARCAL1 expression remains both in the adult neural stem cells in ventricular zone/subventricular zone and mature cortical neurons. **(C)** When SMARCAL1 is deficient, the brain is smaller than normal, possibly because the numbers of adult stem cells may be reduced. Potential impairment in neuronal migration and cortical differentiation can result in histologic features suggestive of lesions such as microdysgenesis and abnormal cortical layering.

hypothesize that the cortical malformations can arise as a consequence of SMARCAL1 dysfunction within the neuronal lineage.

As a member of the swi/snf class of enzymes, SMARCAL1 might alter chromatin structure and/or expression of genes necessary for neural precursor viability or proliferation as well as for effective neuronal migration. Involvement of chromatin remodeling factors in neural precursor renewal has been observed for the mammalian Polycomb group enzyme Bmi-1 (51, 52) and for the Brm-/Brg-1-associated complexes (53–55). Brm-/Brg-1-associated complexes also modulate glial and neuronal differentiation. The murine SWI/SNF (BAF) subunits have nonredundant and dosage-sensitive roles in neural development. Indeed, mice heterozygous for either Brg or BAF155/Srg3 are predisposed to exencephaly (54, 55), and Brg is essential for the repression of neuronal commitment in neural stem cells (56). Furthermore, the transition from proliferating neural stem/progenitor cells to postmitotic neurons requires a switch in subunit composition of the Brm-/Brg-1-associated complexes (53). We postulate that SMARCAL1/Smarcal1 might be a member of other chromatin remodeling complexes that similarly regulate the expression of genes necessary for neural precursor viability and/or renewal as well as for neuronal migration and cortical differentiation. Thus, deficiency of SMARCAL1 would result in a paucity of neural precursors, abnormalities of neuronal migration, and cortical malformations.

A role for SMARCAL1/Smarcal1 in modulating precursor cell renewal and differentiation can also explain the hematopoiesis defects observed in some SIOD patients (9, 10). If SMARCAL1 promotes viability by inhibiting apoptosis of bone marrow stem cells and influences their differentiation along various lineages, this might explain the stem cell factor-resistant bone marrow failure and the high prevalence of T-cell immunodeficiency among SIOD patients (9).

In summary, we have shown for the first time that the disruption of SMARCAL1 expression in patients with SIOD can result in a small brain size, minimal cortical dysgenesis, and other subtle histologic features suggestive of perturbed neuron-glial migration that are often not detected by clinical and magnetic resonance imaging studies. In view of its similarity to other chromatin remodeling proteins, we propose that SMARCAL1 might act as a chromatin chaperone and thereby modulate the expression of a subset of genes involved in neural development.

ACKNOWLEDGMENTS

The authors thank Gabriella D'Arcangelo, Cecilia Ljungberg, Paolo Moretti, R. Grace Zhai, and Millan Patel for critical review of this article; Gabriella D'Arcangelo for advice and support; Barbara A. Antalffy and Pauline Grennan for preparation of tissue; Kyoung Sang Cho for help with confocal microscopy; Monica J. Justice and Darlene Skapura for mouse tissue; Cecilia Ljungberg for technical assistance in setting up the mouse neural stem cell cultures; and the Birth Defects Laboratory at the University of Washington for human brain tissue.

REFERENCES

1. Ohnuma S, Harris WA. Neurogenesis and the cell cycle. Neuron 2003; 40:199–208
2. Temple S. The development of neural stem cells. Nature 2001;414: 112–17
3. Johnson JE. Numb and Numblike control cell number during vertebrate neurogenesis. Trends Neurosci 2003;26:395–96
4. Morshead CM, van der Kooy D. Disguising adult neural stem cells. Curr Opin Neurobiol 2004;14:125–31
5. Gleeson JG, Walsh CA. Neuronal migration disorders: From genetic diseases to developmental mechanisms. Trends Neurosci 2000; 23:352–59
6. Rakic P. Mode of cell migration to the superficial layers of fetal monkey neocortex. J Comp Neurol 1972;145:61–83
7. Angevine JB, Sidman RL. Autoradiographic study of the cell migration during histogenesis of the cerebral cortex in the mouse. Nature 1961; 192:766–68
8. Mochida GH, Walsh CA. Genetic basis of developmental malformations of the cerebral cortex. Arch Neurol 2004;61:637–40
9. Boerkoel CF, O'Neill S, Andre JL, et al. Manifestations and treatment of Schimke immuno-osseous dysplasia: 14 new cases and a review of the literature. Eur J Pediatr 2000;159:1–7
10. Clewing JM, Antalfy BC, Lücke T, et al. Schimke immuno-osseous dysplasia: A clinicopathological correlation. J Med Genet 2007;44: 122–30
11. Boerkoel CF, Takashima H, John J, et al. Mutant chromatin remodeling protein SMARCAL1 causes Schimke immuno-osseous dysplasia. Nat Genet 2002;30:215–20
12. Coleman MA, Eisen JA, Mohrenweiser HW. Cloning and characterization of HARP/SMARCAL1: A prokaryotic HepA-related SNF2 helicase protein from human and mouse. Genomics 2000;65: 274–82
13. Coleman MA, Miller KA, Beernink PT, Yoshikawa DM, Albala JS. Identification of chromatin-related protein interactions using protein microarrays. Proteomics 2003;3:2101–7
14. Kanemura Y, Mori H, Kobayashi S, et al. Evaluation of in vitro proliferative activity of human fetal neural stem/progenitor cells using indirect measurements of viable cells based on cellular metabolic activity. J Neurosci Res 2002;69:869–79
15. Reynolds BA, Weiss S. Generation of neurons and astrocytes from isolated cells of the adult mammalian central nervous system. Science 1992;255:1707–10
16. Kilic SS, Donmez O, Sloan EA, et al. Association of migraine-like headaches with Schimke immuno-osseous dysplasia. Am J Med Genet A 2005;135:206–10
17. Deguchi K, Inoue K, Avila WE, et al. Reelin and disabled-1 expression in developing and mature human cortical neurons. J Neuropathol Exp Neurol 2003;62:676–84
18. Kaneko Y, Sakakibara S, Imai T, et al. Musashi1: An evolutionally conserved marker for CNS progenitor cells including neural stem cells. Dev Neurosci 2000;22:139–53
19. Clewing JM, Fryssira H, Goodman D, et al. Schimke immunoosseous dysplasia: Suggestions of genetic diversity. Hum Mutat 2007;28:273–83
20. Lou S, Lamfers P, McGuire N, Boerkoel CF. Longevity in Schimke immuno-osseous dysplasia. J Med Genet 2002;39:922–25
21. Kandel ER, Schwartz JH, Jessell TM. *Principles of Neuroscience.* 4th ed. New York, NY: McGraw-Hill, 2000
22. Chan C, Moore BE, Cotman CW, et al. Musashi1 antigen expression in human fetal germinal matrix development. Exp Neurol 2006;201:515–18
23. Sakakibara S, Imai T, Hamaguchi K, et al. Mouse-Musashi-1, a neural RNA-binding protein highly enriched in the mammalian CNS stem cell. Dev Biol 1996;176:230–42
24. Frederiksen K, McKay RD. Proliferation and differentiation of rat neuroepithelial precursor cells in vivo. J Neurosci 1988;8:1144–51
25. Wakamatsu Y, Weston JA. Sequential expression and role of Hu RNA–binding proteins during neurogenesis. Development 1997;124:3449–60
26. Sanai N, Tramontin AD, Quinones-Hinojosa A, et al. Unique astrocyte ribbon in adult human brain contains neural stem cells but lacks chain migration. Nature 2004;427:740–44
27. Bansal R, Gard AL, Pfeiffer SE. Stimulation of oligodendrocyte differentiation in culture by growth in the presence of a monoclonal antibody to sulfated glycolipid. J Neurosci Res 1988;21:260–67